Chem Soc Rev

This article was published as part of the

2009 Metal–organic frameworks issue

Reviewing the latest developments across the interdisciplinary area of metal–organic frameworks from an academic and industrial perspective

Guest Editors Jeffrey Long and Omar Yaghi

Please take a look at the issue 5 table of contents to access the other reviews.

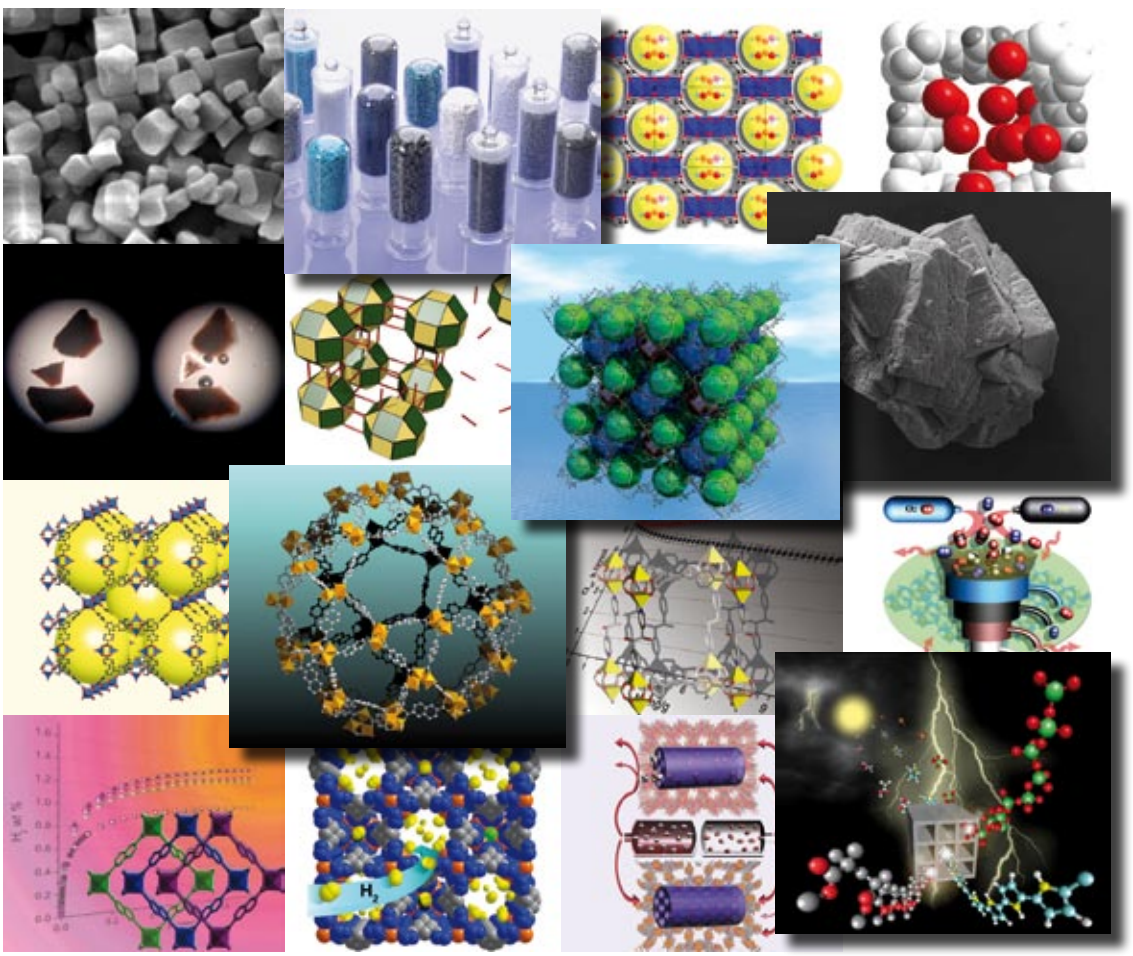

Selective gas adsorption and separation in metal–organic frameworks†

Jian-Rong Li, Ryan J. Kuppler and Hong-Cai Zhou*

Received 30th October 2008
First published as an Advance Article on the web 26th March 2009
DOI: 10.1039/b802426j

Adsorptive separation is very important in industry. Generally, the process uses porous solid materials such as zeolites, activated carbons, or silica gels as adsorbents. With an ever increasing need for a more efficient, energy-saving, and environmentally benign procedure for gas separation, adsorbents with tailored structures and tunable surface properties must be found. Metal–organic frameworks (MOFs), constructed by metal-containing nodes connected by organic bridges, are such a new type of porous materials. They are promising candidates as adsorbents for gas separations due to their large surface areas, adjustable pore sizes and controllable properties, as well as acceptable thermal stability. This *critical review* starts with a brief introduction to gas separation and purification based on selective adsorption, followed by a review of gas selective adsorption in rigid and flexible MOFs. Based on possible mechanisms, selective adsorptions observed in MOFs are classified, and primary relationships between adsorption properties and framework features are analyzed. As a specific example of tailor-made MOFs, mesh-adjustable molecular sieves are emphasized and the underlying working mechanism elucidated. In addition to the experimental aspect, theoretical investigations from adsorption equilibrium to diffusion dynamics *via* molecular simulations are also briefly reviewed. Furthermore, gas separations in MOFs, including the molecular sieving effect, kinetic separation, the quantum sieving effect for H_2/D_2 separation, and MOF-based membranes are also summarized (227 references).

1. Introduction

Selective adsorption occurs when different affinities for different substances on the surface of an adsorbent emerge at given conditions. Separation is a process that divides a mixture into its components.[1,2] Separation can be achieved based on selective adsorption. As the opposite process of mixing, which is favored by the second law of thermodynamics, separation is normally not a spontaneous procedure. Consequently, it often requires major energy consumption, which stimulates many research interests in separation science and technology.[2]

Department of Chemistry, Texas A&M University, College Station, TX 77842-3012, USA. E-mail: zhou@mail.chem.tamu.edu; Fax: (+1) 513-529-0452
† Part of the metal–organic frameworks themed issue.

1.1 General consideration for adsorptive gas separation and purification

Gas separation techniques include cryogenic distillation, membrane-based, and adsorption-based technologies.[1,3] Since the invention of synthetic-zeolites in the 1940s, with the emergence of various adsorbents and the development of adsorption-based separation processes, adsorption has become a key gas separation tool in industry.[4–6] The research activities in adsorption-based gas separation can be traced by the plot in Fig. 1. With the synthesis of more and more new sorbent materials with tailor-made porosity and surface properties and the urgent demand for green separation procedures, adsorptive separation will become increasingly more important. Thus, adsorptive separation will likely play a key role in future energy and environmental technologies.[2,5]

Jian-Rong Li

Jian-Rong "Jeff" Li obtained his PhD in 2005 from Nankai University under the supervision of Prof. Xian-He Bu. Until 2007, he has been an assistant professor at Nankai University. In 2008, he joined Prof. Hong-Cai Zhou's group as a post-doctoral research associate, first at Miami University and currently at Texas A&M University. His recent research interest focuses on metal–organic frameworks and metal–organic supramolecular cages.

Ryan J. Kuppler

Ryan J. Kuppler obtained his Bachelors degree from Miami University in 2008 where since 2005 he was an undergraduate researcher in Prof. Hong-Cai Zhou's group. In 2008 he joined Prof. Zhou's group as a PhD student at Texas A&M University. His research interest focuses on metal–organic frameworks for gas separation and storage.

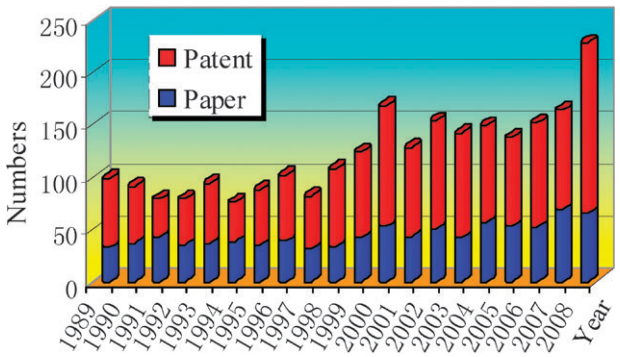

Fig. 1 The development of the field of "gas separation by adsorption" in the last twenty years (SciFinder until Feb. 2009).

Notable examples are H_2 and CH_4 purifications, CO_2 capture, CO removal for fuel cell technology, desulfurization of transportation fuels, and other technologies for meeting the higher environmental standards. A list of the applications in gas separation and purification by adsorption are given in Table 1. Several reviews and monographs on these applications have also appeared.[5,7–15] Conceptually, adsorptive gas separation processes can be divided into two types: bulk separation and purification. The former involves adsorption of a significant fraction (10% or more by weight) from a gas stream, while the latter implies less than 10 wt% adsorption of a gas stream (usually less than 2 wt%).[2]

A general process of adsorptive gas separation or purification includes passing a gas mixture through a column packed with adsorbents or fixed-bed adsorbers to yield a product enriched in the more weakly adsorbed component. This is then followed by desorption of the strongly adsorbed component so that adsorbent can be reused.[2] The high separating power is the result of the continuous contact and equilibration between the gas and adsorbent. A number of such cyclic processes are available depending on the method of the adsorbent regeneration, including thermal swing adsorption (TSA) cycles, pressure swing adsorption (PSA) cycles, inert purge cycles, displacement cycles, and so on. Among them, TSA and PSA are the most commonly used cycles. In a conventional TSA process, desorption is carried out by heating the adsorbent with a portion of the primary gas product. In a PSA cycle, the desorption is achieved by lowering the partial pressures of the adsorbed components in the gas phase by either reducing the total pressure or by flowing a portion of the product gas over the adsorbent without heating. Usually, gas purification is achieved by a TSA process, whereas bulk separation uses a PSA process.[2]

In adsorptive separation processes, gas separation is achieved based on the differences of adsorption capability of different components in the adsorbent. The performance of any such process is directly determined by the characteristics of the adsorbent in both adsorption equilibrium and kinetics.[16,17] The related basic principles of adsorption are described in detail in several monographs.[17–19] In addition to acceptable mechanical properties, a promising adsorbent should possess not only good adsorption capacity and selectivity, but also favorable adsorption kinetics and regenerability. To satisfy these requirements, the adsorbent should first have a reasonably high surface area as well as relatively large pore sizes for porous materials to allow adsorbate molecules to approach the interior surface. For instance, zeolites, with their uniform and somewhat tunable pores, have played a major role in the development of adsorption technology and are widely used in industrial separation.[15,20] Notably, in practical separation processes, adsorbents often require binder materials to provide mechanical strength and to reduce the pressure drop in adsorbent columns. These inert diluents also provide a suitable mesoporous or macroporous structure to facilitate transport of the adsorbate molecules from the external gas phase to the adsorbent pores.[21]

1.2 Porous materials as adsorbents for gas separation and purification

Many porous materials, such as aluminosilicate zeolites, carbon and metal-oxide molecular-sieves, aluminophosphates, activated carbon, activated alumina, carbon nanotubes, silica gel, pillared clays, inorganic and polymeric resins, porous organic materials, and porous metal–organic composites were explored as adsorbents, some of which are now used in industry. Table 2 lists commonly used commercial adsorbents for gas separation and purification. Relevant reviews and monographs have summarized the syntheses, structures, characterizations, adsorption properties, and applications of these materials.[4,15,20,22–25] The adsorption capacity and selectivity of an adsorbent are the principal properties relevant to adsorptive gas separation. The former depends on the equilibrium pressure and temperature, the nature of the adsorbate, and the nature of the micropores in the adsorbent. The latter is significantly more complicated, as it seems to be an integrative and process-related issue in practical separation, though it is still related to the operational temperature and pressure as well as the nature of the adsorbent and the adsorbate.

1.3 Mechanisms of adsorptive separation and adsorbent selections

Gas adsorptive separation by a porous material is usually achieved by one or several of the following mechanisms:[2,26] (1) because of size and/or shape exclusion, certain components of

Hong-Cai Zhou

Hong-Cai "Joe" Zhou obtained his PhD in 2000 from Texas A&M University under the supervision of F. A. Cotton. After a postdoctoral stint at Harvard University with R. H. Holm, he joined the faculty of Miami University, Oxford in 2002. Since the fall of 2008, he has been a professor of chemistry at Texas A&M University. His research interest focuses on hydrogen/methane storage and gas separation that are relevant to clean energy technologies.

Table 1 Selected applications of gas separation and purification[2,13–15]

Application (separation)	Mainly related gas components
Production of O_2 and N_2 enriched air, 90 ~ 93% O_2 for home medical use (air separation, mainly N_2/O_2 separation)	O_2, N_2, CO_2, H_2O, and noble gas
Production of CO_2, CO, and H_2 from steam-methane re-former (SMR) off-gas (SMR off-gas separation)	CO_2, CO, H_2, CH_4, N_2, and H_2O
Production of H_2 from refinery off-gas (ROG) (separation of H_2 and H_2O, C1 ~ C5 alkanes, and alkenes)	H_2, H_2O, C1 ~ C5 alkanes, and alkenes
Production of H_2 from syn-gas (mainly CO/H_2 separation)	H_2 and CO
Solvent vapor recovery (separate H_2O, chlorofluorohydrocarbons, alcohols, ketones, BTX, and N_2 (air))	H_2O, N_2, and other organic solvents
Production of CH_4 and CO_2 from landfill gas (mainly CO_2/CH_4 separation)	CH_4, CO_2, N_2, O_2, and chlorofluorohydrocarbons
Desulfurization from natural gas and transportation fuels	H_2S, COS, N_2 (air), H_2, CH_4, CO_2, H_2O, and organic sulfides
Volatile organic compounds (VOCs) removal	BTX ethyl benzene, alcohols, ketones, chlorinated hydrocarbons, N_2 (air), H_2O, and other organic vapors
Industrial gas drying, H_2O removal	H_2O, N_2, CH_4, CO_2, alcohols, and chlorofuorocarbons
Air brake drying, H_2O removal	H_2O, CO_2, N_2, O_2, and Ar
Electronic gas purification	O_2, N_2, CO, CO_2, NF_3, N_2F_6, SF_6, CF_4, and C_2F_6
Paraffin separation, namely the separation of normal paraffins from isoparaffins and aromatics	All kinds of paraffins, isoparaffins, and aromatics
Xylene separation	*p*-Xylene, *o*-xylene, *m*-xylene, and ethylbenzene
CO_2 removal from blast-furnace gas	CO_2, N_2, O_2, CO, NO_x, SO_2, C_xH_y, and HCl; CO_2, C_xH_y, H_2S, N_2, and He
CO_2 capture from flue gas	CO_2, N_2, O_2, CO, NO_x, SO_2, C_xH_y, and HCl
CO_2/CH_4 and N_2/CH_4 separation for natural gas upgrading	CH_4, N_2, CO_2, C_2H_6, C_3H_8, C_4H_{10}, H_2S, and He
Waste gas treatment in nuclear-related industries, containing NO_x removal and Xe purification	I_2, Kr, NO_x, and Xe
He gas production from the separation of air or natural gas	He, N_2, O_2, CO_2, and H_2O; He, CH_4, CO_2, and N_2
Ne, Ar, Kr, and Xe gas production from the separation of air, or ammonia purge gas	Ne, Ar, Ke, Xe, N_2, O_2, CO_2, and H_2O; Ne, Ar, Ke, Xe, H_2, N_2, CH_4, and NH_3
Removal of silanes from metal hydrides, hydrocarbons and acid gases	SiH_4 and some hydrocarbons or acid gases (such as CO_2, H_2S, and COS)
Flue-gas purification (remove SO_2, NO_x, and HCl from flue gas)	SO_2, NO_x, HCl, N_2, CO_2, O_2, CO, and C_XH_Y
Removal of trace amount of NH_3	NH_3 and other gases
Alcohol dehydration	H_2O and alcohol
Removal of dienes from olefins	Dienes and olefins
Olefin separation	All kinds of olefins
Paraffin/olefin separation	C_2H_4 and C_2H_6; C_3H_6 and C_3H_8; *et al.*
CO_2 and C_2H_4 separation from natural gas	CO_2, C_2H_4, CH_4, C_2H_6, C_3H_8, C_4H_{10}, H_2S, N_2, and He
Gas isotope separation	H_2, D_2, and T_2; ^3He and ^4He

a gas mixture are prevented from entering the pores of an adsorbent while other components are allowed to enter the pores where they are subsequently adsorbed, known as the molecular sieving effect; (2) because of different adsorbate-surface and/or adsorbate packing interactions, preferential adsorption of certain components over others occurs on the surface of an adsorbent, known as the thermodynamic equilibrium effect; (3) because of different diffusing rates, certain components enter the pores and become adsorbed faster than other components, known as the kinetic effect; (4) because of the quantum effect, some light molecules have different diffusing rates in narrow micropores, which allows such molecules to be separated, known as the quantum sieving effect.

Size/shape exclusion, also known as steric separation, is common in zeolites and molecular sieves. For such a given porous adsorbent, both the cross-sectional size (usually referred to as the kinetic diameter or collision diameter, which is defined as the intermolecular distance of the closest approach for two molecules colliding with zero initial kinetic energy) and the shape of the adsorbate molecule are the ultimate factors affecting selective adsorption. It should be pointed out that in some cases temperature also has an impact on molecular sieving if the size of the pore is temperature-sensitive. Two of the most common applications of steric separation are gas drying with 3A zeolite and the separation of normal paraffins from iso-paraffins and other hydrocarbons by using 5A zeolite.[5]

For equilibrium separation, when the pore of the adsorbent is large enough to allow all the component gases to pass, the interaction between the adsorbate and adsorbent surface is crucial in determining the separation quality. The strength of the interaction is decided by the surface characteristics of the adsorbent and the properties of the targeted adsorbate molecule, including but not limited to polarizability, magnetic susceptibility, permanent dipole moment, and quadrupole moment. Table 3 presents a qualitative classification of some gas/vapor adsorbates with respect to their adsorption strength.

When equilibrium separation is not feasible, kinetic separation (also known as "partial molecular sieve action" in its early stage) is another option. One example is air separation using zeolites by PSA. Another example is the production of N_2 from air using a carbon molecular sieve in which O_2 diffuses about 30 times faster than N_2, even though the amounts of both adsorbed at equilibrium are similar. Additional examples include the separation of CH_4 from CO_2 using a carbon molecular sieve, propane/propylene separation by $AlPO_4$-14, and the upgrading of natural gas by the removal of N_2 from CH_4 with 4A zeolite.[2] It has been recognized that for kinetic

Table 2 Comparison of commonly used commercial adsorbents in gas separation and purification[31]

Porous materials	Structure and pore features	Pore size	Application examples
Silica gels	Amorphous, frameworks containing micro- and mesopores with different shapes and sizes, and different degrees of surface hydroxylation	Mean pore diameter: 20 ~ 30 Å	(1) Gas drying; (2) Production of H_2 from ROG
Activated alumina	Amorphous, frameworks containing micro- and mesopores with different shapes and sizes, and pore surfaces containing both basic and acidic sites	Mean pore diameter: 20 ~ 50 Å	(1) Production of O_2 and N_2 enriched air, H_2, CO and CO_2 from SMR off-gas, and H_2 from ROG; (2) Solvent vapor recovery; (3) VOC removal; (4) Electronic gas purification
Activated carbons	Amorphous, frameworks containing interconnected micro- and mesopores with various shapes and sizes, and having different volume fractions and pore walls of different surface chemistry giving rise to different degrees of local surface polarities	Distributed pores with diameter in 3 ~ 100 Å	(1) Production of H_2, CO and CO_2 from SMR off-gas, H_2 from ROG; (2) Solvent vapor recovery; (3) Gas desulfurization; (4) VOC removal
Molecular sieve carbons	Amorphous, microporous frameworks with larger cavities connected by precisely restricted pore windows	Window diameters: 3 ~ 5 Å	(1) Production of O_2 and N_2 enriched air; (2) Production of CH_4 and CO_2 from landfill gas
Zeolites—A, X, chabizite, mordenite, silicalite clinoptilolite, and their ion exchanged forms (H^+, Li^+, Na^+, K^+, Ba^{2+}, Ca^{2+}, Mg^{2+}, Ag^+, *et al.*)	Crystalline, microporous frameworks with well-defined and uniform pore structure in which there exists one or more types of hydrated or non-hydrated cations in different locations, and trace moisture, nonuniform hydrolysis during regeneration	3 ~ 10 Å pore openings: (3A, 3 Å; 4A, 4 Å; 5A, 4.9 Å; NaX, 7.5 Å; CaX, 10 Å; mordenite, 4 Å; chabizite, 4.9 Å; clinoptilolite, 3.5 Å; silicalite, 5.3 Å; Ca and Ba mordenites, 3.8 Å)	(1) Production of O_2 and N_2 enriched air, O_2 from air for home medical use, H_2 and CO_2 from SMR off-gas, CH_4 and CO_2 from landfill gas; (2) Gas drying, desulfurization; (3) Electronic gas purification; (4) Separation of normal paraffins from isoparaffins and cyclic hydrocarbons

Table 3 Qualitative classification of common gases and vapors based on adsorption strength[13]

Adsorption strength	Gas/vapor
Very low	He and H_2
Medium	Ar, O_2, and N_2
High	CO, CH_4, C_2H_6, CO_2, C_3H_8, and C_2H_4
Very high	C_3H_6, C_4H_8, H_2S, NH_3, and H_2O

separation the pore size of the adsorbent needs to be precisely controlled between the kinetic diameters of the two molecules that need to be separated.[2]

In some cases, an adsorbent has narrow micropores to allow light molecules such as H_2, D_2, T_2, and He to penetrate. At low temperatures, when the pore diameter becomes comparable with the de Broglie wave length of these molecules, the quantum sieve effect may allow the separation of such molecules based on the differences in diffusion speeds.[26,27] This effect can be used in isotopic separation. In addition, selectivity may occur based on the differences in desorption rates, known as the desorption effect, which is rare and not fully understood.[28] It should also be pointed out that more than one mechanism can be exploited in certain applications, but in others these mechanisms may prove to be counterproductive.

The situation becomes even more complicated when the porous structure of the adsorbent undergoes a notable structural transformation during adsorption/desorption. This phenomenon is rare and is not always obvious in widely used adsorbents such as zeolites and other molecular sieves because the framework of these materials is usually rigid to some extent. Only at specific conditions, such as high temperature, high pressure, or high polarity of the adsorbate molecules, is it possible for the apertures of these frameworks to undergo an observable change in size and shape.[29,30] Interestingly, some of the recently developed metal–organic framework (MOF) materials have shown this characteristic; the details will be illustrated later.

Adsorbent selection is a complex problem since one must consider both the nature of the adsorption and the process in which the adsorbent is used.[2,31,32] One example lies in purification, where strong adsorption interactions are needed to yield a high Henry's constant, thereby obtaining high purity of the product.[32] In such a situation, adsorbents that form strong interactions with the targeted molecule may be particularly useful. In addition, selection of an adsorbent based on the ease of desorption is also a key criterion for bulk gas separation. When the process is not considered, the adsorbent choice is essentially guided by the size and shape of the adsorbate molecule along with its polarizability, dipole moment, and quadrupole moment. Table 4 gives the adsorption-related physical parameters of selected gas or vapor adsorbates. If the targeted molecule has high polarizability but no polarity, an adsorbent with a high surface area should be a good candidate for adsorption. Adsorbents with highly polarized surfaces are desirable for a targeted molecule with a high dipole moment. If the targeted molecule has a high quadrupole moment, adsorbents with surfaces that have high electric field gradients are ideal.[2] In addition, the formation of weak chemical bonds, such as H-bonds and π-complexation bonds between targeted molecules and adsorbent is also useful for a lot of important separations and purifications. It should also be pointed out that the most important scientific basis for adsorbent selection is the equilibrium isotherm, followed by diffusivity.

Table 4 Physical parameters of selected gas and vapor adsorbates[20,31,33,34]

Adsorbate	Normal BP/K	Liquid V_{mol} at NBP/cm^3 mol^{-1}	T_c/K	V_c/cm^3 mol^{-1}	P_c/bar	Kinetic diameter/Å	Polarizability $\times10^{25}$/cm^3	Dipole moment $\times10^{18}$/esu cm	Quadruple moment $\times10^{26}$/esu cm^2
He	4.30	32.54	5.19	57.30	2.27	2.551	2.04956	0	0.0
Ne	27.07	16.76	44.40	41.70	27.60	2.82	3.956	0	0.0
Ar	87.27	28.7	150.86	74.57	48.98	3.542	16.411	0	0.0
Kr	119.74	34.63	209.40	91.20	55.00	3.655	24.844	0	0.0
Xe	165.01	42.91	289.74	118.00	58.40	4.047	40.44	0	0.0
H_2	20.27	28.5	32.98	64.20	12.93	2.827–2.89	8.042	0	0.662
D_2	23.65	24.81	38.35	60.20	16.65	2.827–2.89	7.954	0	—
N_2	77.35	34.7	126.20	90.10	33.98	3.64–3.80	17.403	0	1.52
O_2	90.17	27.85	154.58	73.37	50.43	3.467	15.812	0	0.39
Cl_2	239.12	45.36	417.00	124.00	77.00	4.217	46.1	0	—
Br_2	331.90	51.51	584.10	135.00	103.00	4.296	70.2	0	—
CO	81.66	35.5	132.85	93.10	34.94	3.690	19.5	0.1098	2.50
CO_2	216.55	37.4	304.12	94.07	73.74	3.3	29.11	0	4.30
NO	121.38	23.4	180.00	58.00	64.80	3.492	17.0	0.15872	—
NO_2 (N_2O_4)	302.22	63.59	431.01	—	101.00	—	30.2	0.316	—
N_2O	184.67	35.9	309.60	97.00	72.55	3.828	30.3	0.16083	—
HCI	188.15	30.6	324.69	81.00	83.10	3.339	26.3–27.7	1.1086	3.8
HBr	206.46	35.85	363.20	—	85.10	3.353	36.1	0.8272	—
CS_2	319.37	—	552.0	173	79.03	4.483	87.4–88.6	0	—
COS	222.7	50.99	378.8	137	63.49	4.130	52–57.1	0.715189	—
SO_2	263.13	44.03	430.80	122.00	78.84	4.112	37.2–42.8	1.63305	—
H_2S	212.84	34.3	373.40	98.00	89.63	3.623	37.82–39.5	0.97833	—
$(CH_3)_2S$	310.48	73.77	503.00	201.00	55.30			1.554	—
NH_3	239.82	25.0	405.40	72.47	113.53	2.900	21.0–28.1	1.4718	—
NF_3	144.11	46.1	234.00	118.75	45.30	3.62	36.2	0.235	—
SF_6	209.25	77	318.72	198.40	37.60	5.128	65.4	0	0
CCl_2F_2	243.45	79	385.10	217.00	41.30	5.0	78.1–79.3	0.51	—
$CHClF_2$	232.14	59.08	369.28	166.00	49.86	—	59.1–63.8	1.42	—
$CHCl_2F$	281.97	75.96	451.52	196.00	51.87	—	68.2	1.29	—
H_2O	373.15	18.8	647.14	55.95	220.64	2.641	14.5	1.8546	—
CH_3OH	337.69	40.73	512.64	118.00	80.97	3.626	32.3–33.2	1.70	—
C_2H_6OH	351.80	58.68	513.92	167.00	61.48	4.530	51.1–54.1	1.69	—
$(CH_3)_2O$	248.31	69.07	400.10	170.00	54.00	4.307	52.9–58.4	1.30	—
Acetone	329.22	73.94	508.10	209.00	47.00	4.600	63.3–64.0	2.88	—
CH_4	111.66	37.8	190.56	98.60	45.99	3.758	25.93	0	0
CH_3Cl	248.95	50.8	416.20	143.00	66.80	4.182	47.2–53.5	1.8963	—
CH_2Cl_2	312.79	65.8	510.00	185	61.00	4.898	64.8–79.3	1.60	—
$CHCl_3$	334.33	84.6	536.50	240.00	55.00	5.389	82.3–95.0	1.04	—
CCl_4	249.79	103.6	556.30	276.00	45.57	5.947	105–112	0	—
CF_4	145.11	53.5	227.51	140.70	37.45	4.662	38.38	0	0
C_2H_6	184.55	55.0	305.32	145.50	48.72	4.443	44.3–44.7	0	0.65
C_2F_6	195.21	86.8	293.04	221.90	30.39	5.10	68.2	0	0
C_2H_4	169.42	49.4	282.34	131.10	50.41	4.163	42.52	0	1.50
C_2H_2	188.40	42.7	308.30	112.20	61.14	3.3	33.3–39.3	0	—
C_3H_8	231.02	75.7	369.83	200.00	42.48	4.3–5.118	62.9–63.7	0.084	—
C_3F_8	236.60	140.00	345.10	299.82	26.80	—	—	0	—
c-C_3H_6	240.34	71.76	398.25	162.80	55.75	4.23–4.807	56.6	0	—
C_3H_6	225.46	69.1	364.90	184.60	46.00	4.678	62.6	0.366	—
n-C_4H_{10}	272.66	96.6	425.12	255.00	37.96	4.687	82.0	0.05	—
i-C_4H_{10}	261.34	97.8	407.85	262.70	36.40	5.278	81.4–82.9	0.132	—
1-Butene	266.92	89.6	419.50	240.80	40.20	4.5	79.7–85.2	0.359–0.438	—
cis-2-Butene	276.87	91.01	435.50	233.80	42.10	4.23	—	0.253	—
trans-2-Butene	274.03	89.6	428.60	237.70	41.00	—	84.9	0	—
1,3-Butadiene	268.62	88.04	425.00	221.00	43.20	5.2	86.4	0	—
n-C_5H_{12}	309.22	118.4	469.70	311.00	33.70	4.5	99.9	0	—
i-C_5H_{12}	300.99	116.46	460.39	308.30	33.81	5.0	—	0.13	—
neo-C_5H_{12}	282.65	122.16	433.75	303.20	31.99	6.2–6.464	102.0	0	—
n-C_6H_{14}	341.88	140.8	507.60	368.00	30.25	4.3	119	0	—
n-C_6F_{14}	329.75	198.91	448.70	573.20	18.70	7	—	0	—
i-C_6H_{14}[a]	333.40	132.89	497.50	366.70	30.10	5.5	—	0.1	—
neo-C_6H_{14}[b]	322.87	133.73	488.70	359.10	30.80	6.2	—	—	—
3-methylpentane	336.40	130.62	504.40	366.70	31.20	5.5	—	—	—
c-C_6H_{12}[c]	353.93	108.75	553.50	308.00	40.73	6.0–6.182	108.7–110	0	—
C_6H_6	353.24	89.41	562.05	256.00	48.95	5.349–5.85	100–107.4	0	—
n-C_7H_{16}	371.57	163.8	540.20	428	27.40	4.3	136.1	0	—
n-C_8H_{18}	398.82	187.5	568.70	492.00	24.90	4.3	159	0	—
i-C_8H_{18}[d]	372.39	184.1	543.90	469.70	25.70	6.2	154.4	0	—
Toluene	383.79	118.2	591.75	316.00	41.08	5.25	118–123	0.375	—
o-Xylene	417.59	121.25	630.30	370.00	37.32	6.8	141–149	0.640	—

Table 4 (*continued*)

Adsorbate	Normal BP/K	Liquid V_{mol} at NBP/cm^3 mol^{-1}	T_c/K	V_c/cm^3 mol^{-1}	P_c/ bar	Kinetic diameter/Å	Polarizability $\times10^{25}$/cm^3	Dipole moment $\times10^{18}$/esu cm	Quadruple moment $\times10^{26}$/esu cm^2
m-Xylene	412.34	123.47	617.00	375.00	35.41	6.8	142	0.37	—
p-Xylene	411.53	123.93	610.20	378.00	35.11	5.8	137–149	0.1	—
Ethylbenzene	409.36	123.08	617.15	374.00	36.09	5.8	142	0.59	—

[a] 2-Methylpentane. [b] 2,2-Dimethylbutane. [c] Cyclohexane. [d] 2,2,4-Trimethylpentane.

1.4 Characterizations of adsorptive separation

Experimentally, at a given temperature, the adsorption quantity of a gas can be measured by an adsorption isotherm which is generally carried out by one of two methods: volumetric or gravimetric. The adsorption isotherm (namely equilibrium isotherm) characterizes the adsorption equilibrium, which is the foundation for the evaluation of adsorptive separation. The equilibrium isotherm is also the predominant scientific basis for adsorbent selection. The studies of isosteric heat, as well as adsorption and diffusion kinetics, such as using various breakthrough experiments, are also important. The diffusion of a single adsorbate can be characterized by two distinct diffusivities: self-diffusivity $D_s(c)$ and transport diffusivity $D_t(c)$. The former measures the displacement of a tagged molecule as it diffuses inside an adsorbent at a specified concentration c at equilibrium. Macroscopic diffusion in a crystalline material is usually characterized by the transport diffusivity, which is defined as the proportionality constant relating a macroscopic flux J to a macroscopic concentration gradient ∇c: $J = -D_t(c)\nabla c$. The adsorption behaviors of a gas mixture on an adsorbent are very complicated. The usual procedure for the adsorption characterization of a gas mixture is to circulate a gas mixture through a column or bed of adsorbents until the equilibrium is established. An experimental breakthrough curve is usually used to characterize the separation of a gas mixture. For a gas mixture, the separation factor S provides a numerical value for selectivity. The selectivity for component A relative to component B is defined by $S = (x_A/x_B)(y_B/y_A)$, where x_A and x_B are the mole fractions of components A and B in the adsorbed phase and y_A and y_B are the mole fractions of A and B in the bulk phase. In experiments, the gas-chromatographic method and fixed-bed adsorption are usually used to evaluate the separation of a gas mixture.

Commonly used materials for gas separation and purification in industry are mainly limited to four types: activated carbon, zeolites, silica gel, and activated alumina. Future applications of adsorptive separation depend on the availability of new and better adsorbents. "Ideally, the adsorbent should be tailored with specific attributes to meet the needs of each specific application".[2] Exploitation of better adsorbents, especially those easily tailored, can thus improve the performance of the current industrial processes. In the past two decades, we have witnessed an explosion in the research and development of new porous materials, the spearhead being porous MOFs, which have great application potential in gas separation and purification as adsorbents.

2. Metal–organic frameworks and their potential application in gas separation by selective adsorption

Porous materials encompass a wide range of adsorbents.[25,35–44] Some of them, with zeolites being the first to come to mind, are structurally uniform with well-defined pore sizes and shapes, whereas others are less structurally-defined containing pores with a wide variety of sizes. In the past decade, a new class of synthetic porous materials, metal–organic frameworks (MOFs),[45–47] also called porous coordination polymers (PCPs),[48] porous coordination networks (PCNs),[49] or other names,[50] have been developed into one of the most prolific areas of research in chemistry and materials (Fig. 2). MOFs are inorganic–organic hybrid materials comprised of single metal ions or polynuclear metal clusters linked by organic ligands principally through coordination bonds (Fig. 3 presents three examples for the construction of MOFs[51–53]). Due to the strength of these coordination bonds, MOFs are geometrically and crystallographically well-defined framework structures. In most cases, these structures are robust enough to allow the removal of the included guest species resulting in permanent porosity. The crystallinity of MOFs also allows precise structural characterization by diffraction methods, thus facilitating their rational design and the formulation of structure-function relationships. MOFs can be conceptually designed and assembled based on how building blocks come together to form a net, termed as reticular synthesis by Yaghi and coworkers.[54] As a result, the structures and properties of MOFs can be well-designed and systematically tuned by the judicious choice of metal-based building blocks and organic linkers, which can be readily regulated by employing the power of organic synthesis.[39,55–66] This remarkable tunability is quite different from that of traditional porous zeolites whose pores are confined by rigid tetrahedral oxide skeletons that are usually difficult to alter. It

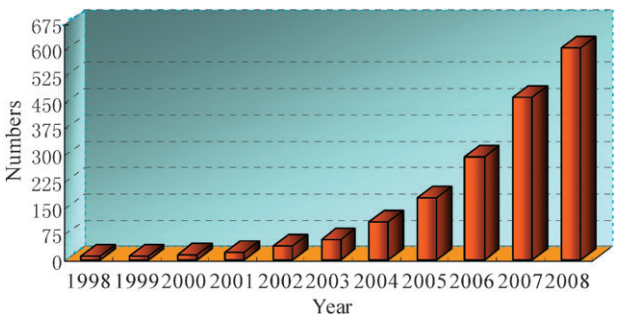

Fig. 2 Number of publications *vs.* year for metal–organic Frameworks (SciFinder until Feb. 2009).

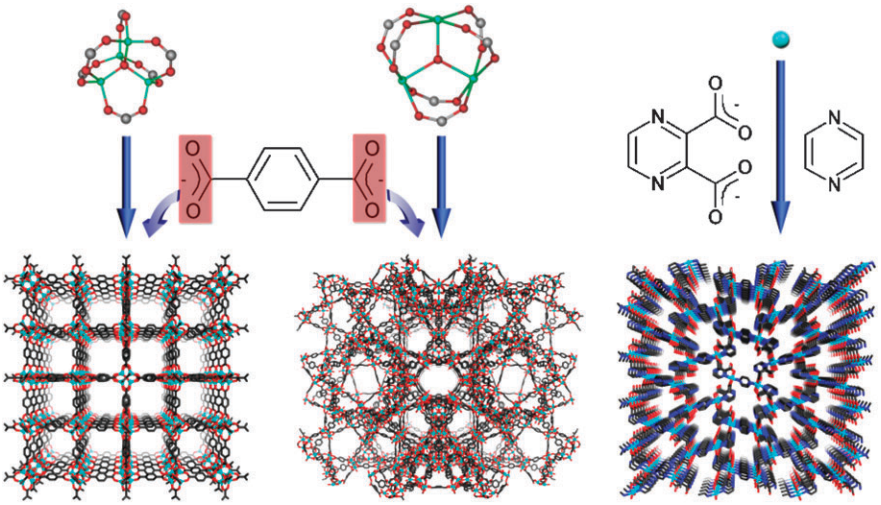

Fig. 3 Schematic representation of the construction of MOFs.[51–53]

allows facile optimization of the pore structure, surface functional groups, and other properties for specific applications. MOFs can be made with exceptionally high porosity and are typically synthesized by a simple self-assembly reaction between various metal ions and organic linkers under mild conditions. Consequently, MOFs are ideal for research and practical applications, such as in gas separation and purification as adsorbents.[67,68]

Arbitrarily, MOFs can be categorized into rigid and flexible/dynamic classes. Rigid MOFs have comparatively stable and robust porous frameworks with permanent porosity, similar to zeolites and other inorganic porous materials, whereas flexible MOFs possess dynamic, "soft" frameworks that respond to external stimuli, such as pressure, temperature, and guest molecules.[40,69–72] This extraordinary sensitivity to external stimuli affords MOFs specific properties such as pressure/temperature dependent molecular sieving, which is beyond the scope of traditional adsorbents such as zeolites and activated carbons. While the initial focus in the field of MOFs was the synthesis and structural characterization, an increasing number of MOFs are now being explored for their interesting properties, including optic,[57,73–77] magnetic,[78–84] and electronic properties,[85–89] as well as their various potential applications such as catalysis,[90–94] ion exchange,[50,77,95–97] gas storage,[98–104] separation,[105–108] sensing,[109–112] polymerization,[113–115] and drug delivery.[116–118] MOFs are ideal adsorbents for gas storage and separation due to their large surface areas, adjustable pore sizes, and controllable surface properties. As shown in Fig. 4, selective gas adsorption and separation represents one of the most active research areas in MOF research. As potential adsorbents in gas separation and purification, MOFs offer unique advantages for specific applications based on their structural characteristics.[119] As discussed above, gas separation is a complicated process. The development of a new adsorbent in industry normally goes through multiple steps such as materials design and preparation, selective gas adsorption studies, materials evaluation, adsorbents preparation scale-up, and separation process design and optimization. Currently, the investigation of MOFs as adsorbents in gas separation is in its early stage. Most of the research is focused on selective gas adsorption studies based on adsorption/desorption isotherm measurements of single gas components, which provide the predominant information for adsorbent screening.

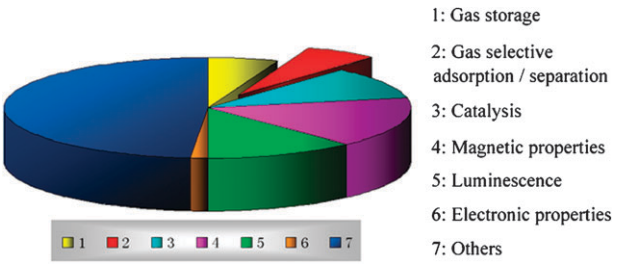

Fig. 4 The ratio of the research on the topic of "selective gas adsorption and/or separation" in the MOFs field (SciFinder until Feb. 2009).

3. Selective gas adsorption in rigid metal–organic frameworks

So far, tens of thousands of MOFs have been synthesized and structurally characterized; however, only a few hundred of them have been tested for their adsorption properties. Selective adsorption has been observed in less than about seventy MOFs, mostly based on gas adsorption isotherms. In rigid MOFs, much like in zeolites, the adsorption selectivity may be related to the molecular sieving effect and/or preferential adsorption based on the different strengths of the adsorbent–adsorbate and adsorbate–adsorbate interactions. Fig. 5 presents a schematic illustration of selective gas adsorption in rigid MOFs. Different from that of flexible MOFs, rigid MOFs frequently exhibit type I isotherms. A survey of selective gas adsorption in rigid MOFs has been given in Table 5.

3.1 Selective adsorption based on size/shape exclusion

Selective adsorption based mainly on the molecular sieving effect has been confirmed in several MOFs. Structural analysis revealed that manganese formate has a robust 3D framework structure with 1D channels.[121] These channels contain larger

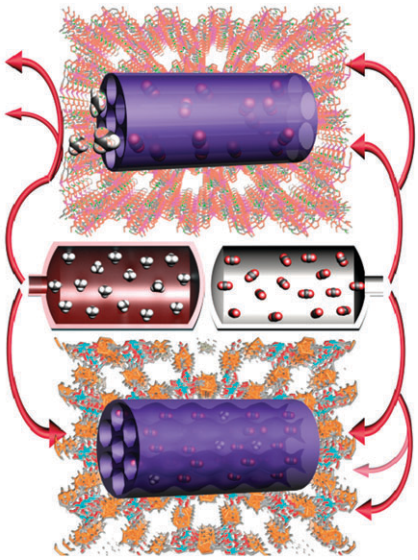

Fig. 5 Schematic illustration of selective gas adsorption in rigid MOFs (top: the molecular sieving effect, bottom: preferential adsorption).

cages, which are connected to each other *via* a small window. Gas sorption experiments indicated that at 78 K this material can selectively adsorb H_2 over N_2 and Ar, and at 195 K CO_2 over CH_4. In both cases, the adsorption capacities of the excluded gases N_2, Ar, and CH_4 were almost zero. Thus, the selectivity was attributed to the small aperture of the channels. The selective adsorption of H_2 but not N_2 due to size exclusion was also observed in $Mg_3(ndc)_3$,[123] PCN-13,[131] $Sm_4Co_3(pyta)_6(H_2O)_x$,[133] $Cu(F\text{-}pymo)_2$,[139] and $Zn_2(cnc)_2(dpt)\cdot Guest$[143] at 77 K as shown in Table 5. Recently, we reported a coordinatively linked interpenetrated MOF, PCN-17,[145] which has a porous structure containing large cages linked by relatively small apertures and retains its porosity at temperatures as high as 480 °C. The interpenetration and sulfate bridging in PCN-17 reduce its pore (window) size to approximately 3.5 Å leading to selective adsorption of H_2 and O_2 over N_2 and CO (Fig. 6). This material may thus have applications for the separation of N_2 and O_2, the separation of H_2 from CO in fuel-cell applications, as well as the H_2 enrichment of the N_2/H_2 exhaust. MIL-96[127] and $Zn_2(cnc)_2(dpt)$[143] were also found to selectively adsorb CO_2 over CH_4 based on size/shape exclusion. These materials may be useful in the separation of CO_2 and CH_4, which is an essential industrial process for natural-gas purification and landfill-gas separation. It should be pointed out that in some systems the activation temperature of the sample has important effects on the pore sizes, as observed in $Zn_2(cnc)_2(dpt)\cdot Guest$ and its guest-free counterpart.[143] The former has the ability to selectively adsorb H_2 over N_2 whereas the latter adsorbs CO_2 over CH_4. It is also interesting to note that MOFs $Mg_3(ndc)_3$,[123] Zn(dtp),[138] and PCN-13[131] have the ability to selectively adsorb O_2 but not N_2 at low temperatures due to the pore size exclusion effect, even though the two molecules are similar in size as shown in Table 4. In addition, the selective adsorption of H_2O over MeOH vapor was observed in $Cu(gla)(4,4'\text{-bipy})_{0.5}$.[142]

A very important potential application for the selective vapor adsorption is the separation of hydrocarbons. Indeed this has been achieved in $Cu(hfipbb)(H_2hfipbb)_{0.5}$,[125] which was characterized by both molecular simulations and experimental studies. The channels in this material consist of alternating elliptical, large chambers and narrow windows with a suitable size, which leads to the selective adsorption of normal C_4 over higher normal alkanes and olefins at room and higher temperatures due to both shape and size exclusions.

3.2 Selective adsorption based on adsorbate–surface interactions

Although the pore size and shape of an adsorbent are the major factors in determining the adsorption selectivity of guest molecules as discussed above, the nature of the guest-surface interaction is also important. In some of the rigid MOFs, the reported adsorption selectivity can be attributed to the thermodynamic equilibrium effect or the kinetic effect in a given equilibrium time, namely the preferential adsorption but not the molecular sieving effect. In these cases, the selectivity was demonstrated to be related to adsorbate properties such as polarity, quadruple moment, and H-bonding, as well as to the surface properties of the pores. A unique selective adsorption of C_2H_2 over CO_2 was achieved by $Cu_2(pzdc)_2(pyz)$ (Fig. 7).[124] To obtain C_2H_2 with high purity, it is crucial to separate C_2H_2 from a gas mixture containing CO_2. It is difficult to use zeolites and activated carbons to achieve this task because these two molecules are very similar in size and other sorption-related physical properties. $Cu_2(pzdc)_2(pyz)$ has a porous structure containing 1D open channels of 4×6 Å in cross-section size. The surface of the channels contains O atoms, which can act as basic adsorption sites for guest molecules. The sorption isotherms of both gases at 270, 300, and 310 K showed that this MOF can adsorb C_2H_2 more favorably than CO_2 at low pressure and ambient temperature. Further investigations indicated that C_2H_2 bound stronger to the surface than CO_2 due to H-bonding between C_2H_2 molecules and the surface O atoms of the MOF. Similar selective adsorption of C_2H_2 over CO_2 was also observed in microporous MOFs $Mn(HCOO)_2$ and $Mg(HCOO)_2$ at room temperature.[122] Herein, the discrimination of the two molecules was attributed to the slightly larger size of C_2H_2 relative to CO_2, which was believed to provide the former with more-effective van der Waals interactions with the framework walls. Similarly, based on potential H-bonding, $Zn_2(bptc)$ was found to selectively adsorb $CHCl_3$, MeOH, and H_2O but not hexane and pentane at 298 K.[130] This material also showed adsorption selectivity of benzene and toluene over hexane and pentane at room temperature, presumably due to $\pi\cdots\pi$ interactions between the adsorbed molecules and aromatic rings in the pore surface. Selective adsorption based on the hydrophobic/hydrophilic properties of pores has also been observed in $Cu(hfipbb)(H_2hfipbb)_{0.5}$,[125] Zn(tbip),[128] and $Zn(bdc)(ted)_{0.5}$.[134] The three MOFs have hydrophobic channels of larger than 4.0 Å. Adsorption isotherms of these MOFs showed the selective adsorption of organic solvents such as MeOH, EtOH, and dimethylether over water. In two additional examples, $Cd_3(OH)_2(apt)_4(H_2O)_2$[132] and CUK-1,[136,137] channels inside the MOFs are

Table 5 Summary of selective gas adsorption in rigid MOFs

MOF[a]	Pore features	Pore size/Å[b]	Pore V/ cm^3 g^{-1}[c]	Adsorption selectivity	Uptake (T, P)	Reason[d]	Ref.
$Er_2(pda)_3$	1D circular channel with coordinatively unsaturated Er^{III} sites	~3.4	0.05	CO_2 over N_2 and Ar	CO_2, ~24 mg g^{-1} (273 K, 760 torr) N_2 and Ar, almost none (77 K, 760 torr)	A and B	120
$Mn(HCOO)_2$	1D circular channel with alternating large chambers and small windows (or 1D zigzag channel) interconnected by small apertures	~4.5 (~3.64[e])	0.19~0.22	H_2 over N_2 and Ar	H_2, ~100 mL g^{-1} (78 K, 1 atm) N_2 and Ar, almost none (78 K, 1 atm)	A and/or B	121
				CO_2 over CH_4 and N_2	CO_2, ~105 mL g^{-1} (195 K, 1 atm) CH_4 and N_2, almost none (195 K, 1 atm)		122
				C_2H_2 over CO_2, CH_4, N_2, O_2, and H_2	C_2H_2, ~51.2; CO_2, ~36; CH_4, ~14 mL g^{-1}; N_2, O_2, and H_2, almost none (298 K, 760 torr)		122
$Mg_3(ndc)_3$	1D elliptical channel with coordinatively unsaturated Mg^{II} sites	3.46~3.64	0.62	O_2 and H_2 over N_2 and CO	O_2, ~3.5 mmol g^{-1} (77 K, 880 torr) H_2, ~2.3 mmol g^{-1} (77 K, 880 torr) N_2 and CO, almost none (77 K, 880 torr)	A	123
$Cu_2(pzdc)_2(pyz)$	1D rectangular channel with exposed basic O adsorption sites	4 × 6	0.09	C_2H_2 over CO_2	C_2H_2, ~42 mL g^{-1} (270 K, 4.5 kPa) CO_2, ~3 mL g^{-1}(270 K, 4.5 kPa)	B	124
$Cu(hfipbb)(H_2hfipbb)_{0.5}$	1D near circular channel with hydrophobic internal surface, and alternating oval-shaped large chambers and narrow windows	3.2 and 7.3	0.072	C_2, C_3, n-C_4 olefins and alkanes over all branched alkanes and all normal hydrocarbons above C_4	Propane, 2.6 wt% (0.062 P/P°) Propene, 2.0 wt% (0.019 P/P°) n-mutane, 4.0 wt% (0.33 P/P°) 2-methylpropane, n-pentane, 3-methylbutane, n-hexane, and 3-methylpentane, 0% (298 K)	B	125
				MeOH over H_2O	MeOH, 2.0 wt% (298K, 0.6 P/P°) H_2O, almost none (298 K)	B	
$Cr^{III}_3O(H_2O)_2F(ntc)_{1.5}$ (MIL-102)	1D circular channel with coordinated terminal water molecules and decorated by F^- anions	4.4	—	CO_2 over CH_4 and N_2	CO_2, ~3.4 mmol g^{-1} (304 K, 3 MPa) CH_4, ~1.4 mmol g^{-1} (304 K, 2.8 MPa) N_2, ~1 mmol g^{-1} (304 K, 2.6 MPa)	B	126
$Al_{12}O(OH)_{18}(H_2O)_3[Al_2(OH)_4](btc)_6$ (MIL-96)	Three types of cages connected by small widows	2.5~3.5	0.32	CO_2 over CH_4	CO_2, ~3.7 mmol g^{-1} (303 K, 3.5 bar) CH_4, ~0.8 mmol g^{-1} (303 K, 3.5 bar)	A	127
Zn(tbip)	1D circular hydrophobic channel	4.5	0.12	MeOH over H_2O	MeOH, 110 mg g^{-1} (298 K, 0.73 P/P°) H_2O, <1 mg g^{-1} (298 K, 0.65 P/P°)	B	128
				DME over MeOH	DME, 30 mg g^{-1} (303 K, 0.73 P/P°)		
Cu(bdt)	1D channel with unsaturated coordination sites	—	0.72	O_2 over N_2 and H_2	O_2, ~14 mmol g^{-1} (77 K, 0.9 P/P°) N_2 and H_2, <3 mmol g^{-1} (77 K, 0.9 P/P°)	B	129
$Zn_2(bptc)$	Two types of interconnecting pores with H-bond based O atoms and aryl planes suitable for π···π stacking	3.9 × 5.1 (5.2)	0.19	$CHCl_3$, MeOH, H_2O, benzene, and toluene over hexane and pentane	Ether, ~13 wt%; $CHCl_3$, ~24 wt%; MeOH, ~10 wt%; Benzene, ~9 wt%; Toluene, ~13 wt%, H_2O, 15 wt%; Pentane, 7 wt%; hexane, 8.5 wt% (298 K, 1 P/P°)	B	130
$Zn_4O(H_2O)_3(adc)_3$ (PCN-13)	1D square hydrophobic channel	3.5 × 3.5	0.30	H_2 and O_2 over N_2 and CO	O_2, ~68 mL g^{-1} (77 K, 1 P/P°) H_2, ~46 mL g^{-1} (77 K, 1 P/P°) N_2 and CO, ~10 mL g^{-1} (77 K, 1 P/P°)	A	131
$Cd_3(OH)_2(apt)_4(H_2O)_2$	1D square channel with high electric field	5.4 × 5.4	0.12	H_2 and CO_2 over N_2	H_2, ~68 mL g^{-1} (77 K, 0.90 atm) CO_2, ~67 mL g^{-1} (195 K, 0.92 atm) N_2, almost none (77 K, 1 atm)	B	132
$Sm_4Co_3(pyta)_6(H_2O)_x$ (x < 9)	1D ellipsoid channel with coordinatively unsaturated metal sites	3.5 × 5.0	0.08	H_2 and CO_2 over N_2	H_2, ~20 mL g^{-1} (77 K, 1 P/P°) CO_2, ~45 mL g^{-1} (195 K, 1 P/P°) N_2, almost none (77 K, 1 P/P°)	A	133

Table 5 (*continued*)

MOF[a]	Pore features	Pore size/Å[b]	Pore V/ cm^3 g^{-1}[c]	Adsorption selectivity	Uptake (T, P)	Reason[d]	Ref.
$Zn(bdc)(ted)_{0.5}$	Two types of 1D interconnected hydrophobic channels	7.5 × 7.5 3.2 × 4.8	0.69	MeOH and EtOH over H_2O	MeOH, 5.02 mg g^{-1} (0.42 P/P°) EtOH, 418 mg g^{-1} (0.42 P/P°) H_2O, <10 mg g^{-1} (0.42 P/P°) (298 K)	B	134
$Zn_4O(btb)_2$ (MOF-177)	Large cages connected by small windows	7.1 ~ 7.6	1.31	O_2 over N_2	O_2, 0.18 mmol g^{-1} (298 K, 1 atm) N_2, 0.10 mmol g^{-1} (298 K, 1 atm)	B	135
$Co_3(u_3\text{-}OH)_2(2,4\text{-}pdc)_2$ (CUK-1)	1D diamond-shaped channels with corrugated walls	11.1	0.28	O_2 and H_2 over N_2 and Ar CO_2 over CH_4	O_2, ~130 mL g^{-1} (87 K, 470 torr) H_2, ~180 mL g^{-1} (77 K, 760 torr) N_2 and Ar, almost none (77 K, 1 atm) CO_2, ~88 mL g^{-1} (298 K, 760 torr) CH_4, <10 mL g^{-1} (298 K, 760 torr)	B	136 137
$Mg(HCOO)_2$	1D zigzag channels interconnected by small apertures	~4.7 (~3.36[e])	0.21	C_2H_2 over CO_2, CH_4, N_2, O_2, and H_2	C_2H_2, ~66; CO_2, ~45; CH_4, ~15 mL g^{-1}; N_2, O_2, and H_2, almost none (298 K, 760 torr)	B	122
Zn(dtp)	1D N-rich chiral channels	4.1	0.29	O_2 and CO_2 over N_2	O_2, ~79 mL g^{-1} (77 K, 1 atm) CO_2, ~99 mL g^{-1} (195 K, 1 atm) N_2, almost none (77 K, 1 atm)	A	138
$Cu(F\text{-}pymo)_2$	1D helical channel with O atoms decorated surface	2.9	0.06	H_2 over N_2	H_2, ~79 mL g^{-1} (77 K, 900 torr) N_2, almost none (77 K, 900 torr)	A	139
Zn(bIM)(nIM) (ZIF-68)	Large cages connected by relative small apertures	7.5	0.46	CO_2 over CO	CO_2, ~65; CO, ~7 mg g^{-1} (STP) (273 K, 760 torr)	B and different critical point of the gases	140
Zn(cbIM)(nIM) (ZIF-69)		4.4	0.30		CO_2, ~67; CO, ~4 mg g^{-1} (STP) (273 K, 760 torr)		
$Zn(IM)_{1.13}(nIM)_{0.87}$ (ZIF-70)		13.1	0.57		CO_2, ~52; CO, ~4 mg g^{-1} (STP) (273 K, 760 torr)		
$Zn(cbIM)_2$ (ZIF-95)	Large cages connected by small apertures	3.65	0.59	CO_2 over CH_4, CO and N_2	CO_2, ~0.87; CH_4, ~0.27; CO, ~0.103; N_2, ~0.08 mmol g^{-1} (298 K, 850 torr)	A and B	141
$Zn_{20}(cbIM)_{39}(OH)$ (ZIF-100)	Large cages connected by small apertures	3.35	—	CO_2 over CH_4, CO and N_2	CO_2, ~0.95; CH_4, ~0.28; CO, ~0.105; N_2, ~0.075 mmol g^{-1} (298 K, 850 torr)	A and B	141
$Cu(gla)(4,4'\text{-}bipy)_{0.5}$	1D hydrophobic elliptical channel	3.3 × 5.1	0.11	H_2O over MeOH	H_2O, ~5.1 mmol g^{-1} (298 K, 0.96 P/P°) MeOH, ~2.1 mmol g^{-1} (298 K, 0.96 P/P°)	A	142
$Zn_2(cnc)_2(dpt)\cdot$Guest	Triangular 1D channels	<3.7	0.13	H_2 over N_2	H_2, ~117 mL g^{-1} (77 K, 1 P/P°) N_2, none (77 K, 1 P/P°)	A	143
$Zn_2(cnc)_2(dpt)$	Triangular 1D channels	~3.7	0.27	CO_2 over CH_4	CO_2, ~150 mL g^{-1} (195 K, 1 P/P°) CH_4, ~80 mL g^{-1} (195 K, 1 P/P°)	A and B	143
Mn(ndc)	Rhombic 1D channels with coordinatively unsaturated Mn^{II} sites	~4	0.40	CO_2 over CH_4	CO_2, ~1.5 mmol g^{-1} (273 K, 1 atm) CO_2, ~3.0 mmol g^{-1} (195 K, 1 atm) CH_4, ~0.8 mmol g^{-1} (273 K, 1 atm) CH_4, ~1.7 mmol g^{-1} (195 K, 1 atm)	B	144
$Yb_4(\mu_4\text{-}H_2O)(tatb)_{8/3}(SO_4)_2$ (PCN-17)	Large cages connected by small apertures	3.5	0.32	H_2 and O_2 over N_2 and CO	O_2, ~210 mL g^{-1} (77 K, 1 P/P°) H_2, ~105 mL g^{-1} (77 K, 1 P/P°) N_2 and CO, ~20 mL g^{-1} (77 K, 1 P/P°)	A	145
$Zn_3(OH)(p\text{-}cdc)_{2.5}$	Intersecting rhombic channels with coordinatively unsaturated Zn^{II} sites	3 × 5	~0.6	CO_2 over CH_4	CO_2, ~0.586 mmol g^{-1} (298 K, 0.5 bar) CH_4, ~0.0754 mmol g^{-1} (298 K, 0.5 bar)	B	146

Table 5 (*continued*)

MOF[a]	Pore features	Pore size/Å[b]	Pore V/ cm^3 g^{-1}[c]	Adsorption selectivity	Uptake (T, P)	Reason[d]	Ref.
$Zn_3(OH)(p\text{-cdc})_{2.5}(DMF)_3$	1D square channels	3 × 6	~0.3	CO_2 over CH_4	CO_2, ~0.277 mmol g^{-1} (298 K, 0.5 bar) CH_4, ~0.0682 mmol g^{-1} (298 K, 0.5 bar)	B	146
$Co(HCOO)_2$	1D zigzag channels interconnected by small apertures	~5	~0.2	Ethylbenzene over *p*-xylene	Ethylbenzene, ~120 mg g^{-1} (313 K, 6 torr) *p*-xylene, ~32 mg g^{-1} (313 K, 6 bar)	B	147
$Zn_2(ndc)_2(dpni)$	Intersecting rhombic channels	4 ~ 5	—	CO_2 over CH_4	CO_2, ~4.3 mmol g^{-1} (296 K, 1750 kPa) CH_4, ~2.5 mmol g^{-1} (296 K, 1750 kPa)	B	148

All terms are taken directly from the original literature unless noted. [a] Abbreviations: pda = 1,4-phenylendiacetate, ndc = 2,6-naphthalenedicarboxylate, pzdc = pyrazine-2,3-dicarboxylate, pyz = pyrazine, H_2hfipbb = 4,4′-(hexafluoroisopropylidene)bis(benzoic acid), ntc = naphthalene-1,4,5,8-tetracarboxylate, btc = 1,3,5-benzenetricarboxylate, tbip = 5-*tert*-butylisophthalicate, bdt = 1,4-benzeneditetrazolate, bptc = 4,4′-bipyridine-2,6,2′,6′-tetracarboxylate, adc = 9,10-anthracenedicarboxylate, apt = 4-aminophenyltetrazolate, pyta = 2,4,6-pyridinetricarboxylate, bdc = 1,4-benzenedicarboxylate, ted = triethylenediamine, btb = 1,3,5-benzenetribenzoate, 2,4-pdc = pyridine-2,4-dicarboxylate, dtp = 2,3-pyrazinedithiotrazolate, F-pymo = 5-fluoropyrimidin-2-olate, IM = imidazolate, nIM = 2-nitroimidazolate, cbIM = 5-chlorobenzimidazolate, pyenH_2 = 5-methyl-4-oxo-1,4-dihydro-pyridine-3-carbaldehyde, 4,4′-bipy = 4,4′-bipyridine, gla = glutarate, cnc = 4-carboxycinnamic, dpt = 3,6-di-4-pyridyl-1,2,4,5-tetrazine, tatb = 4,4′,4″-*S*-triazine-2,4,6-triyltribenzoate; *p*-cdc = 1,12-dicarba-*closo*-dode-caborane-1,12-dicarboxylate, DMF = dimethylformamide, dpni = *N*,*N*′-di-(4-pyridyl)-1,4,5,8-naphthalene tetracarboxydiimide. [b] The size was obtained from either a crystal structure or molecular simulations, in some cases before activation. The numerical values correspond to the pore shapes: for a circular or near circular pore, its diameter is provided; for others, the length of a side is given. It represents the aperture with the minimal dimension in cage-containing systems. Dimensions denote those excluding the van der Waals radius if possible. [c] The pore volume was approximately evaluated by PLATON based on crystal data, in which some of the solvent molecules were removed before calculation. [d] Probable reason for selective adsorption: A, size/shape exclusion; B, different adsorbent–adsorbate interactions. [e] This number is provided by the authors in their subsequent publication: "The diameter corresponds to that of the largest probe atom, which can be fitted to the narrowest part of the channel based on the X-ray crystal structure at 90 K. Calculated with Materials Studio modeling software."[149]

larger than all of the adsorbed gas molecules. The former selectively adsorbed H_2 and CO_2 but not N_2, and the latter adsorbed O_2 and H_2 over N_2 and Ar at low temperatures. These selectivities were also attributed to the preferential adsorption by authors.

Several MOFs can selectively adsorb CO_2 over CH_4 because CO_2 has a large quadrupole moment whereas CH_4 has none. For instance, $Zn_2(ndc)_2(dpni)$ is a pillared-layer MOF synthesized by using a microwave heating method.[148] The adsorption isotherms of this MOF indicated that CO_2 was more preferentially adsorbed than CH_4. In the same report, a molecular simulation of a binary mixture adsorption showed that this material has an adsorption selectivity factor of ~30 for CO_2 over CH_4. Another example, Mn(ndc) is a 3D microporous MOF with 1D channels in which there exist coordinatively unsaturated Mn^{II} sites.[144] The adsorption measurements showed that this MOF has much higher adsorption capabilities for CO_2 than for CH_4 at ambient temperatures. Similar selective adsorption of CO_2 over CH_4 has also been confirmed by Snurr and coworkers in a carborane-based MOF with coordinatively unsaturated metal sites by a comparison of experimental results with molecular simulations.[146] These results have shown that open metal sites in a MOF can aid in the separation of (quadru) polar/non-polar gas pairs such as CO_2/CH_4. Furthermore, the adsorption of CO_2 over CH_4 was evaluated recently in an extrudates material with $Cu_3(btc)_2$ MOF as the adsorbent.[150] The results showed that this material has adsorption selectivity of 4 ~ 6 for CO_2 over CH_4 at the pressure range of 0.1 ~ 3 bar and high CO_2 adsorption capacity (6.6 mol kg^{-1} at 2.5 bar and 303 K). Thus, this MOF-based material may have a potential application in vacuum PAS units for CO_2/CH_4 separation.

It is also of interest that recently developed zeolitic imidizolate frameworks (ZIFs) have shown high CO_2 storage ability and can capture CO_2 from CO_2/CO mixtures.[140] These frameworks contain large cages interconnected by small apertures. For example, in ZIF-68, 69, and 70, the large cages have diameters of 7.2, 10.2, and 15.9 Å, which are connected by apertures of sizes 4.4, 7.5, and 13.1 Å, respectively. At 273 K, the CO_2 and CO adsorption isotherms showed that all of these ZIFs have a high affinity and capacity for CO_2. The selective adsorption was further confirmed by breakthrough experiments, which showed complete retention of CO_2 and passage of CO when they were exposed to a stream containing a 50:50 v/v binary mixture of CO_2 and CO at room temperature. Besides the different critical points (as listed in Table 4) of the two gases, which have a large influence on adsorption, this selectivity can be attributed to the equilibrium effect based on different quadruple moments of CO_2 and CO, but not the molecular sieve effect because the pores in these ZIFs are large enough to allow both gas molecules to enter. Similar explanations were used in $Co(HCOO)_2$ for its selective adsorption of ethylbenzene over *p*-xylene.[147] As a result, such gas mixtures may be separated *via* an equilibrium-based process. In addition, at normal atmospheric pressure and 298 K, MOF-177 showed adsorption selectivity for O_2 over N_2; this was attributed to the higher magnetic susceptibility of O_2 than that of N_2.[135]

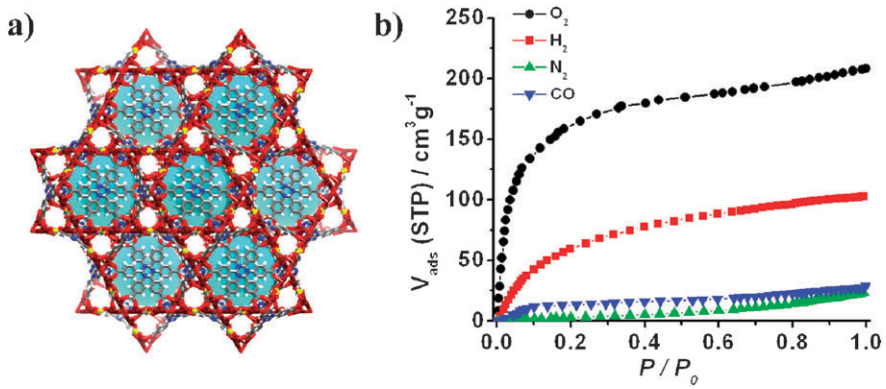

Fig. 6 (a) Structure of PCN-17 with aqua spheres showing large cages in the framework. (b) Adsorption isotherms of the activated PCN-17 at 77 K.[145]

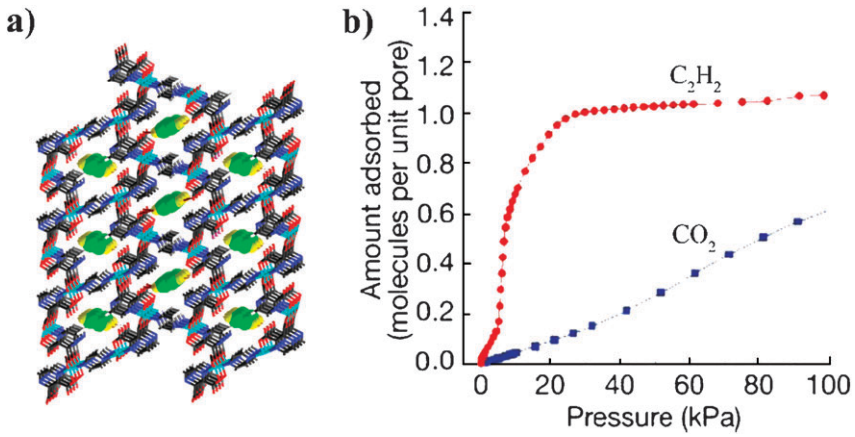

Fig. 7 (a) Structure of $Cu_2(pzdc)_2(pyz)$ with C_2H_2 (green-yellow, space-filling model) at 170 K. (b) Adsorption isotherms on $Cu_2(pzdc)_2(pyz)$ at 300 K.[124]

3.3 Selective adsorption based on cooperative effects of size/shape exclusion and adsorbate–surface interactions

The selective gas adsorption in some MOFs seems to be related to both the pore size and the interactions between adsorbate molecules and the pore walls. One example is $Er_2(pda)_3$,[120] which has a 3D framework structure with 1D circular channels and coordinatively unsaturated Er^{III} sites. The effective dimension of the channels is approximately 3.4 Å in diameter. Adsorption measurements showed selective adsorption of CO_2 over Ar and N_2, which was attributed to the combined effects of size and of host–guest interactions by the authors. It was suggested that the host framework, with its coordinatively unsaturated Er^{III} ions, polar groups, and π-electrons, may give rise to an electric field, inducing a dipole in CO_2. Besides the induced dipole interaction, the quadrupole moment of CO_2 would interact with the electric field gradient, contributing further to the adsorption potential energy. In addition, a possible donor–acceptor affinity between the Er^{III} ions and the CO_2 molecules was also proposed. Other examples are two recently reported ZIFs, ZIF-95 and 100 (Fig. 8),[141] both having unique combinations of large cavities and highly constricted apertures of 3.65 and 3.35 Å in the largest dimension, respectively. At room temperature, both ZIFs showed a high affinity and storage capacity for CO_2 over CH_4, CO, and N_2. The high selectivity for CO_2 was ascribed to the combined effects of the size of the pore apertures being similar to CO_2 and the strong quadrupolar interactions of CO_2 with N atoms present on the pore surface, whereas it is also relevant to the higher critical point of CO_2 than those of other gases.

In addition, it should also be noted that for the same MOF, the adsorption properties may be distinct at different temperatures. One such example is $Mn(HCOO)_2$.[121,122] As discussed above, at low temperatures, this MOF exhibited selective adsorption of H_2 over N_2, whereas at room temperature, no selectivity was found for the two gases.

As demonstrated above, rigid MOFs have great application potential in gas separations because both their pore size and shape and their surface properties can be easily tuned by the selection of metal or metal clusters, ligand design and functionalization, as well as by post-synthetic modification. For molecular sieving to occur, it is essential to use restricted small pores. For example, by utilizing a short bridging ligand, porous manganese formate was synthesized and its gas adsorption selectivity was observed.[121] Increasing the bulkiness of the ligands to constrict the apertures of porous MOFs was also proven to be effective in PCN-13 in our lab.[131] In addition, interpenetration is another well-known and effective

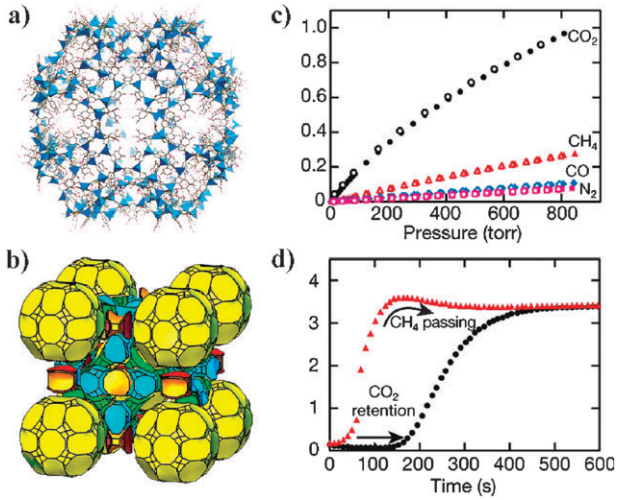

Fig. 8 (a) Structure of a large cage in ZIF-100. (b) Natural tiling of ZIF-100 with the giant cages being in yellow. (c) Gas adsorption/desorption isotherms of ZIF-100 at 298 K. (d) Breakthrough curves of CH_4 (red) and CO_2 (black) for ZIF-100 using a $V_{1:1}$ CH_4/CO_2 gas mixture.[141]

way to reduce the pore size of a MOF. This has recently been used to confine the pore size for selective adsorption of gas molecules.[143] Most of the interpenetrated MOFs reported are flexible to some extent, which will be discussed later. In terms of surface properties, the uncoordinated nitrogen atoms distributed throughout the pore surfaces of some ZIFs were suggested to induce a polar pore wall which was proposed to be responsible for the favorable CO_2 adsorption. These ZIFs were obtained by using N-functionized ligands, 4-azabenzimidazolate, purinate, and 5-azabenzimidazolate as linkers.[141] In addition, one of the emerging strategies to modify the MOF surface is to introduce coordinatively unsaturated metal sites. This has been demonstrated in the selective adsorption of CO_2 over CH_4 in several MOFs.[144,146]

4. Selective gas adsorption in flexible/dynamic metal–organic frameworks

Before discussing the selective adsorption behaviors of MOFs with flexibility, it is necessary to clarify the flexibility in zeolites. Recent theoretical studies showed that all zeolites possess some framework flexibility over a density range.[151] Therefore, it is not uncommon that some zeolites can adsorb molecules with diameters larger than their pore size under specific conditions. For example, it is known that bulky aromatic molecules with diameters of 9.0 and 9.5 Å can be adsorbed into zeolite NaX with a nominal pore diameter of 7.4 Å.[29] In most practical cases the flexibility of the pores is related to the lattice flexibility of the zeolite, as demonstrated experimentally.[30] Similarly, several theoretical simulations have also been performed to elucidate the influence of the flexibility of zeolite frameworks on their adsorption properties and diffusion kinetics.[152,153] Evidently, in some cases the flexibility plays an important role in gas adsorptive separation using zeolites. However, flexibility in zeolites usually occurs only at high temperatures and/or pressures, and the change of lattice and aperture is minor because zeolite frameworks are constructed with strong covalent bonds that are rigid.[154] It should be pointed out that this flexibility is different from those triggered by solvent removal, which leads to zeolite frameworks with different pore sizes.[155,156] In addition, in some cases the free counterions inside frameworks can adjust their positions under certain conditions, resulting in frameworks that may have different responses to different adsorbates.[157] All of these should be discriminated from the flexibility of dynamic MOFs.

For MOFs, the entire framework is supported by coordination bonds and/or other weak cooperative interactions such as H-bonding, π–π stacking, and van der Waals interaction. The flexibility is thus expected even under mild conditions.[71] So far, many flexible MOFs have been synthesized but only a few were characterized by adsorption. During the adsorption/desorption procedure, such MOFs are not well-defined structurally and the actual porous structure responsible for the uptake/leaving of the adsorbates may result from guest directed framework transformations (Fig. 9). With the flexibility of the framework, such MOFs often exhibit selective adsorption. Table 6 lists results published in this area, together with the proposed mechanisms for framework flexibility and the suggested reasons of gas adsorption selectivity. Comparatively, the selective gas adsorption in flexible MOFs is more complicated than that in rigid MOFs. In most cases, the sorption isotherms show hysteretic behaviors due to framework rearrangements during adsorption-desorption processes. Besides size/shape exclusion and adsorbate-surface

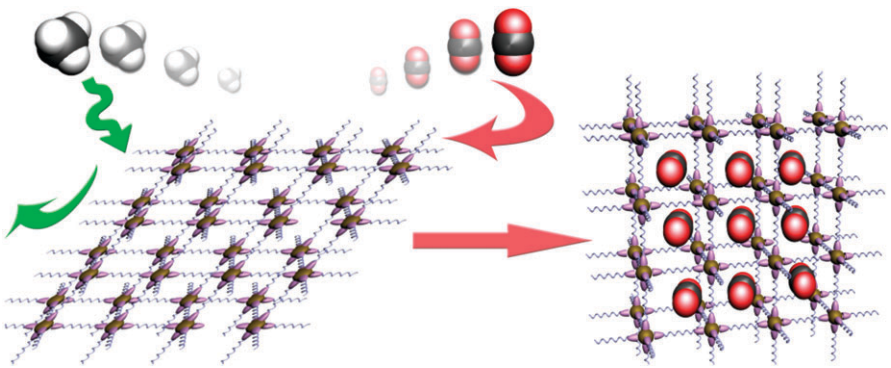

Fig. 9 Schematic illustration of selective gas adsorption in a flexible MOF.

Table 6 Summary of selective gas adsorption in flexible/dynamic MOFs

MOF[a]	Structural features	Adsorption conditions		Selective adsorption	Uptake	Dynamic mechanism[b]	Reason for selectivity[c]	Ref.
		T/K	P					
$Cu(dhbc)_2(4,4'\text{-bpy})$	Interdigitated 2D framework, stacking through π–π interactions to form 1D channels	298	0.4 ~ 8 atm	CO_2 over CH_4, O_2, and N_2	CO_2, ~70 mL g^{-1}	A	C	158
			10 ~ 35 atm	CO_2 and CH_4 over O_2 and N_2	CO_2, ~80 mL g^{-1} CH_4, ~67 mL g^{-1}			
			35 ~ 50 atm	CO_2, CH_4, and O_2 over N_2	CO_2, ~82; CH_4, ~73; O_2, ~45 mL g^{-1}			
$Cu(bdc)(4,4'\text{-bpy})_{0.5}$	Interpenetrated 3D pillared-layer framework with intersecting 1D potential open channels	276 ~ 298	0.1 ~ 0.2 MPa	CO_2 over CH_4, O_2, and N_2	CO_2, ~70 mL g^{-1}	A	C	158
			0.9 ~ 2.9 MPa	CO_2 and CH_4 over O_2 and N_2	CO_2, ~95 mL g^{-1} CH_4, ~60 mL g^{-1}			159
			2.9 ~ 3.2 MPa	CO_2, CH_4, and O_2 over N_2	CO_2 ~98 mL g^{-1} CH_4 ~70 mL g^{-1} O_2 ~50 mL g^{-1}			
$Cu_2(pzdc)_2(dpyg)$	3D pillared-layer framework with flexible and OH functional pillars and 1D channels	298	$P > 0.23\ P/P^\circ$	CH_3OH over CH_4	CH_3OH, 6.2 mmol g^{-1} at 0.5 P/P°	B	D	160
Cd(pzdc)(bpee)	3D pillared-layer framework with 1D channels decorated by protruded C = O groups	298	~1.0 P/P°	H_2O and MeOH over EtOH, THF, and Me_2CO	H_2O, 68 mL g^{-1} MeOH, 35 mL g^{-1} EtOH, THF, and Me_2CO, almost none	B	A	161
M(OH)(bdc) M = Al, Cr (MIL-53)	3D framework with 1D diamond-shaped channels containing H-bonding sites	304	30 bar	CO_2 over CH_4	CO_2, ~10 mmol g^{-1} CH_4, ~6 mmol g^{-1}	B	B	162
Cu(pyrdc)(bpp)	2D pillared-bilayer framework without pores	77 for N_2 and O_2 195 for CO_2 298 for MeOH and EtOH		N_2 and O_2 cannot be adsorbed at all CO_2, MeOH, and EtOH can be adsorbed at different relative pressures		A	C	163
Cr(OH)(bdc)-H_2O (MIL-53)	3D framework with 1D diamond-shaped channels containing H-bonding sites	304	20 bar	CO_2 over CH_4	CO_2, ~7.5 mmol g^{-1} CH_4, almost none	B	B	164
$Zn(adc)(4,4'\text{-bpe})_{0.5}$	Interpenetrated 3D pillared-layer framework with intersecting 1D potential open channels	77	1 P/P°	H_2 over N_2 and CO	H_2, ~70 mL g^{-1} N_2 and CO, almost none	B	A	165
		195	1 P/P°	CO_2 over CH_4	CO_2, ~130 mL g^{-1} CH_4, almost none			
$H_2Ni_3O(H_2O)_3(tatb)_2 \cdot 2H_2O$ (PCN-5)	Interpenetrated 3D framework stabilized by H-bonding with three types of intersecting 1D channels in three directions	195	760 torr	CO_2 over CH_4	CO_2, ~210 mg g^{-1} CH_4, ~30 mg g^{-1}	B	A	166
$Zn(Pur)_2$ (ZIF-20)	3D framework with large cages connected by small distensible apertures	273	760 torr	CO_2 over CH_4	CO_2, ~70 mL g^{-1} CH_4, ~15 mL g^{-1}	C	D	167
$Cd(4\text{-btapa})_2(NO_3)_2$	Interpenetrated 3D framework with channels functionalized by amide groups	298 for MeOH 77 for N_2	0.9 P/P° 0.9 P/P°	MeOH over N_2	MeOH, 130 mL g^{-1} N_2, almost none	B	D	168
$[Ni(bpe)_2(N(CN)_2)](N(CN)_2)$	Interpenetrated 3D framework with bimodal functionality	195 for CO_2 and Xe 77 for O_2 and N_2	1 P/P° 1 P/P°	CO_2 over O_2, N_2, and Xe	CO_2, ~35 mL g^{-1} O_2, N_2, and Xe, almost none	B	B	169
		298	0.9 P/P°	H_2O and MeOH over EtOH and Me_2CO	H_2O, ~110 mL g^{-1} MeOH, ~85 mL g^{-1} EtOH and Me_2CO ~32 mL g^{-1}		B	

Table 6 (*continued*)

MOF[a]	Structural features	Adsorption conditions		Selective adsorption	Uptake	Dynamic mechanism[b]	Reason for selectivity[c]	Ref.
		T/K	*P*					
Ce(tci)	3D nonporous framework	298 for H_2O and MeOH 195 for CO_2, 77 for N_2	—	H_2O over MeOH, CO_2, and N_2	H_2O, 4 molecules/host unit MeOH, CO_2, and N_2 almost none	D	B (coordination)	170
$Co(ndc)(4,4'\text{-bipy})_{0.5}\cdot(Guest)_x$	Interpenetrated 3D pillared-layer framework with intersecting 1D potential open channels	Sample activated at 150 °C, 77	0.5 P/P°	H_2 over N_2	H_2, ~80 mL g^{-1} N_2, ~40 mL g^{-1}	B	A	171
		Sample activated at 200 °C, 77	0.5 P/P°		H_2, ~65 mL g^{-1} N_2, ~5 mL g^{-1}			
$Cu(fma)(4,4'\text{-bpe})_{0.5}$	Interpenetrated 3D pillared-layer framework with intersecting 1D potential open channels	77	1 P/P°	H_2 over CO, Ar, and N_2	H_2, 92 mL g^{-1} CO, Ar, and N_2, almost none	B	A	172
		195	760 torr	CO_2 over CH_4 and N_2	CO_2, 100 mL g^{-1}; CH_4, 35 mL g^{-1}; N_2, 15 mL g^{-1}			
Cd(bpndc)(4,4′-bpy)	Interdigitated 2D framework, stacking with H-bonding to form 0D cavities	90	4~40 kPa	O_2 over N_2 and Ar	O_2, ~145 mL g^{-1}	A	C	173
			40~55 kPa	O_2 and Ar over N_2	O_2, 150 mL g^{-1}; Ar, 90 mL g^{-1}			
$Ni_2(cyclam)_2(mtb)$	Interpenetrated 3D framework with wide inside pockets connected by narrow entrances	77 for H_2, N_2, and O_2 195 for CO_2 and CH_4		H_2, CO_2, and O_2 over N_2 and CH_4	H_2, 79 mL g^{-1} at 1 atm CO_2, 57 mL g^{-1} at 1 atm O_2, 25 mL g^{-1} at 0.19 atm N_2 and CH_4, <10 mL g^{-1} at 0.9 atm	C	A	174
Cu(etz)	3D framework with large cages connected by small hydrophobic changeable apertures	298	1 P/P°	MeOH, EtOH, and MeCN over H_2O	MeOH, ~175 mg g^{-1} EtOH, ~245 mg g^{-1} MeCN, ~220 mg g^{-1} H_2O, almost none	B and C	B	175
				C_6H_6 over C_6H_{12}	C_6H_6, ~200 mg g^{-1} C_6H_{12}, almost none		A	
$Ln(tci)(H_2O)$	3D framework with 1D channels with ligand having highly flexible arms and secondary functional groups	298	0.9 P/P°	H_2O and MeOH over EtOH, THF, and Me_2CO	H_2O, 8 molecules/unit MeOH, 2 molecules/unit EtOH, THF, and Me_2CO, almost none	B	A	176
				MeOH over MeCN	MeOH, 2 molecules/unit MeCN, almost none		B	
$Zn_2(tcom)(4,4'\text{-bpy})$	Interpenetrated 3D PtS-type framework with intersecting channels	298	1 bar	CO_2 over H_2 and N_2	CO_2, 5wt% H_2 and N_2, almost none	B	B	177
$Ag_2[Cr_3O(OOCC_2H_5)_6(H_2O)_3]_2[\alpha\text{-}SiW_{12}O_{40}]$	Nonporous layer ionic framework with exposed Ag^+ sites	298 or 301	50~400 KPa	Small unsaturated hydrocarbons over paraffins and larger unsaturated hydrocarbons	Unsaturated hydrocarbons, ≥ 1.0 mol/mol Paraffins and larger unsaturated hydrocarbons, almost none	B	D	178

All terms obtained directly from the original literature, unless specified otherwise. [a] Abbreviation: dhbc = 2,5-dihydroxybenzoate, pzdc = pyrazine-2,3-dicarboxylate, dpyg = 1,2-di(4-pyridyl)glycol, bpee = 4,4′-(*E*)-ethene-1,2- diyldipyridine, pyrdc = pyridine-2,3-dicarboxylate, bpp = 1,3-bis(4-pyridy)propane, 4,4′-bpe = *trans*-bis(4-pyridyl)ethylene, Pur = purinate, 4-btapa = 1,3,5-benzenetrcarboxylic acid tris[N-(4-pyridyl)amide], tci = 3,3′,3″-(2,4,6-trioxo-1,3,5-triazinane-1,3,5-triyl)tripropionate, bpndc = benzophenone-4,4′-dicarboxylate, cyclam = 1,4,8,11-tetraazacyclo-tetradecane, mtb = methanetetrabenzoate, etz = 3,5-diethyl-1,2,4-triazolate, $tciH_3$ = tris(2-carboxyethyl)isocyanurate, H_2tcom = tetrakis[4-(carboxyphenyl)oxamethyl]methane, and refer to Table 5. [b] Probable framework dynamic mechanisms: A, pressure induced, guest molecule triggered structure transformation process; B, host–guest interaction based, guest molecule triggered structural transformation process; C, guest molecule triggered dynamic aperture-widening process; D, pressure induced, guest molecule coordinated topochemical transformation process. [c] Probable reason for selective adsorption: A, size/shape exclusion; B, different guest–adsorbate interactions. C, different guest-dependent gate-opening pressures; D, host–guest interaction induced gate-opening.

interaction, structural rearrangement must also be taken into account. Based on the structural features of flexible MOFs and adsorption characteristics, selective gas adsorption in flexible MOFs can be classified into the following four categories.

4.1 Selective adsorption based on size/shape exclusion accompanied by pore size/shape change

The gas adsorption selectivity in some flexible MOFs can be attributed to the size/shape exclusion effect, despite the change of the pores upon adsorption. This has been observed in Cd(pzdc)(bpee),[161] in which the Cd(pzdc) layers are pillared through the axial Cd coordination of bpee to form a 3D framework with 1D channels. Adsorption studies revealed that at 298 K this MOF adsorbs H_2O and MeOH, accompanied by channel expansion, but not EtOH, THF, and Me_2CO, suggesting that the adsorption selectivity arises from the molecular sieving effect. In Ln(tci)(H_2O),[176] similar adsorption selectivity was observed at 298 K. Size-exclusion based adsorption selectivity was also found in flexible Cu(etz),[175] which has a porous structure with large cavities interconnected by small apertures with pendant ethyl groups in open space. This MOF can selectively adsorb benzene over cyclohexane. In addition, selective adsorption based on pore sizes has also been observed in a series of interpenetrated pillared-layer flexible MOFs listed in Table 6. Fig. 10 presents the structure and gas adsorption isotherms of such a typical example, Cu(fma)(4,4′-bpe)$_{0.5}$.[172] Except for PCN-5,[166] their frameworks are typically composed of paddlewheel dinuclear M_2 units that are bridged by dicarboxylate dianions to form a 2D layer, which are further pillared by bipyridine type ligands in the third dimension. When adsorbates enter the pores, these interpenetrated frameworks can alter their pore sizes through the adjustment of inter-framework distances. Systematic tuning of the dicarboxylate and bi-pyridine type ligands has led to a series of this type of MOF, indicating that the "rational design" approach is useful in tuning the micropores of such MOFs for their separation of gas molecules by taking advantage of framework interpenetration.[172] With the richness of dicarboxylates and bridging bidentate organic ligands with variable lengths, more flexible interpenetrated MOFs are expected to be constructed to meet the specific needs of separation applications.

4.2 Selective adsorption based on adsorbate–surface interactions accompanied by pore size/shape change

Similar to that in rigid MOFs, the surface property of pores also plays a critical role in determining adsorption selectivity of flexible MOFs for different gases. This has been observed in MIL-53[162,164] in both its dehydrated and hydrated forms. MIL-53 has a 3D structure containing 1D diamond-shaped channels of approximately 8.5 Å in dimension evaluated in its hydrated form (Fig. 11a). This material exhibited a breathing phenomenon upon hydration–dehydration. In its hydrated form the pores are slightly deformed due to hydrogen-bonding interactions between H_2O molecules and the O atoms of the carboxylate and the hydroxo groups. It is interesting to note that dehydrated MIL-53 showed different adsorption behaviors for CH_4 and CO_2 (Fig. 11b).[162] The adsorption isotherm of CH_4 was typical for a microporous material, whereas the CO_2 isotherm exhibited two steps; above the first step at low pressure the CO_2 adsorption capacity greatly exceeded that of CH_4. The difference between the CH_4 and CO_2 isotherms was attributed to the quadrupole moment of the CO_2 molecules. For the hydrated MIL-53,[164] the adsorption isotherm of CO_2 showed very little uptake at pressures up to 10 bar, while a distinct high uptake occurred in the 12 ~ 18 bar pressure range. However, the adsorption isotherm of CH_4 showed almost no uptake below 20 bar. This was attributed to the repulsive effect of the water molecules in the host framework and the nonpolar CH_4 molecules. Another

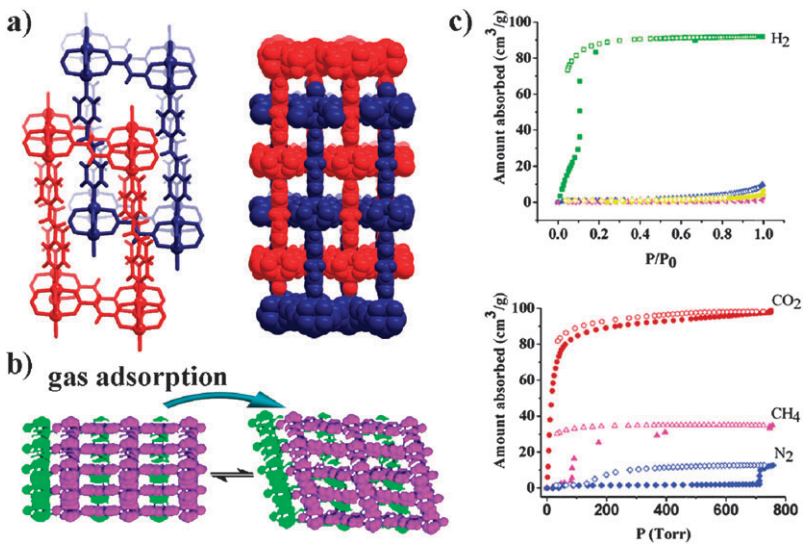

Fig. 10 (a) Structure of Cu(fma)(4,4′-bpe)$_{0.5}$ showing doubly interpenetrated cubic nets and corresponding pore void spaces. (b) Schematic illustration of possible framework transformation during gas adsorption on Cu(fma)(4,4′-bpe)$_{0.5}$. (c) Gas adsorption/desorption isotherms of Cu(fma)(4,4′-bpe)$_{0.5}$ at (up) 77 K (N_2, blue; Ar, magenta; CO, yellow) and (down) 195 K.[172]

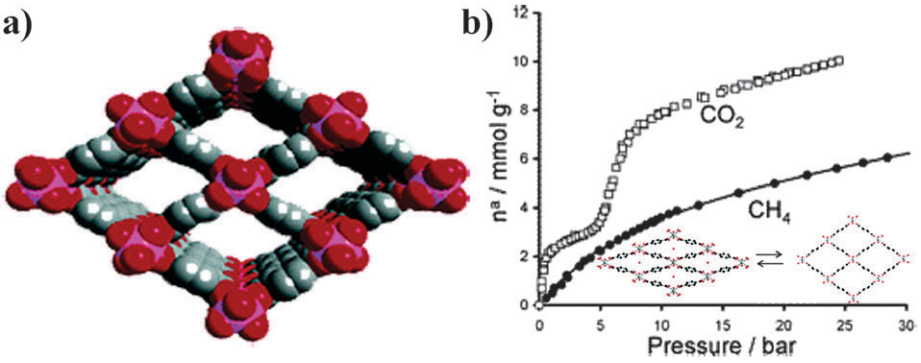

Fig. 11 (a) Framework structure of MIL-53. (b) Gas adsorption isotherms of MIL-53(Cr) at 304 K (inset, schematic illustration of the "breathing" effect in MIL-53(Cr)).[162]

example is the selective adsorption of MeOH over MeCN at room temperature in Ln(tci)(H_2O).[176] This MOF has a 3D porous structure with hydrophilic channels whose surfaces are decorated by uncoordinated O atoms in the ligands and metal-coordinated water molecules. Despite the comparable sizes of MeOH and MeCN molecules, only MeOH molecules can enter the channels. This was attributed to the fact that MeOH molecules can form strong H-bonds with the O donors on the pore surface, whereas MeCN cannot. The adsorption characteristics observed in $[Ni(bpe)_2(N(CN)_2)](N(CN)_2)$[169] seem to be more complicated. This material has a stable interpenetrated 3D framework structure with 1D channels. Even though the pore size is adequately large, O_2 and N_2 cannot diffuse into the micropores, whereas CO_2, MeOH, H_2O, EtOH, and acetone molecules can. All the isothermals showed hysteretic sorption behavior, corresponding to a dynamic structural transformation from guest-free to guest-filled forms. This unusual adsorption selectivity was accounted for by the strong interactions of O_2 or N_2 with the pore windows at 77 K, which blocks other molecules from passing into the pore. In the case of CO_2 (at 195 K), these interactions were suggested to be overcome by the thermal energy and the strong interaction between CO_2 molecules and framework host. It was also proposed that the Ni^{II} atoms, the functional groups, and the π-electron clouds of the bpe ligands inside the pores gave rise to an electric field, which was effective in the adsorption of CO_2 due to its high quadrupole moment. For the adsorption of MeOH, H_2O, EtOH, and acetone vapor, H-bonding interactions between these molecules and the host framework were suggested to be responsible.

4.3 Selective adsorption based on gate-opening or structural rearrangement induced by adsorbate–surface interactions

In their closed state, some flexible MOFs have small or even no pores to allow guest entrance. However, the pores expand when exposed to certain gas adsorbates in what is known as the gate-opening process. Whether or not the expansion occurs depends on the adsorbate-surface interactions. The selective adsorption of CO_2 over CH_4 was observed in ZIF-20,[167] which has a 3D porous structure with large cages connected by small windows. At 273 K, the CO_2 uptake at 760 torr is five times higher than that of CH_4 suggesting a stronger interaction between the pore surface and the CO_2 molecules. It is interesting to note that the maximum pore aperture (2.8 Å as measured from the crystal structure) of ZIF-20 is smaller than the kinetic diameter of CO_2 and CH_4. Therefore, it was believed that the large cage space in the structure becomes accessible through a dynamic window-widening process wherein the ligands swing to allow gas molecules to pass. This result demonstrated that molecules with dipole and quadrupole moments seem to have a distinct effect on the framework flexibility of some MOFs. The formation of H-bonds is also the driving force of gate openings as observed in $Cu_2(pzdc)_2(dpyg)$,[160] which has a 3D framework structure composed of 2D $Cu_2(pzdc)_2$ layers pillared by dpyg ligands. The framework provides narrow 1D channels in which –OH groups of the dpyg ligands are exposed and have the potential to form H-bonds with guest molecules. The adsorption isotherms of MeOH and H_2O vapors, as well as CH_4 at 298 K, have revealed that MeOH or H_2O was adsorbed when the pressure was increased to a certain value, but that no CH_4 was adsorbed. In addition, the desorption isotherm did not trace the adsorption isotherm indicating the occurrence of a framework transformation. Herein the selective adsorption exhibited by $Cu_2(pzdc)_2(dpyg)$ can primarily be associated with the H-bonding interaction between the MeOH or H_2O molecules and the –OH groups of the dpyg ligands. This attractive force is strong enough to transform the channel structure to allow the entrance of the guest molecules. A similar adsorption behavior has also been observed in $Cd(4\text{-btapa})_2(NO_3)_2$,[168] a 3D interpenetrating framework with exposed amide groups acting as guest-interacting sites on the surfaces of the open channels as shown in Fig. 12. Gas adsorption studies and XRPD measurements showed that this material selectively adsorbs guest molecules with a concurrent structural transformation from amorphous to crystalline. At 77 K, no N_2 uptake was observed; however, MeOH vapor can be adsorbed at 298 K with the sorption profile showing large hysteresis. Further investigation confirmed that the amide groups on the channel surfaces provide an attractive interaction with the MeOH molecules *via* H-bonding, and the interaction is strong enough to transform the channel structure. In addition, the hydrophobicity/hydrophilicity of the channel surfaces can also direct the adsorption selectivity. For example, Cu(etz) can selectively adsorb organic molecules

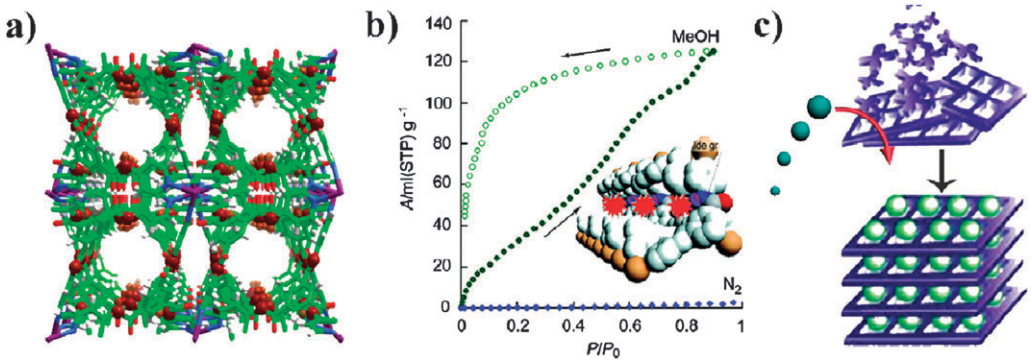

Fig. 12 (a) Structure of $Cd(4\text{-btapa})_2(NO_3)_2$ with NO_3^- anions omitted and amide groups highlighted by maroon spheres. (b) Gas adsorption/desorption isotherms of $Cd(4\text{-btapa})_2(NO_3)_2$ for N_2 (at 77 K) and MeOH (at 298 K) (inset, potential strong adsorption sites (amide groups) on the channel surface of $Cd(4\text{-btapa})_2(NO_3)_2$). (c) Schematic representation of the structural transformation from amorphous to crystalline induced by adsorption in $Cd(4\text{-btapa})_2(NO_3)_2$.[168]

such as MeOH, EtOH, and MeCN but not H_2O, due to the kinetically controlled flexibility and its hydrophobic pore surface.[175] On the contrary, Ce(tci) has a 3D structure with no channels, yet it selectively adsorbs H_2O vapor but rejects other vapor or gas adsorbates such as MeOH, EtOH, acetone, THF, N_2, and CO_2.[170] When the adsorption of H_2O vapor was carried out, a change in the host framework structure was observed from a 3D nonporous framework to a 2D sheet compound. Such a material may be useful in drying organic solvents. Another reported nonporous MOF with gas adsorption selectivity is $Ag_2[Cr_3O(OOCC_2H_5)_6(H_2O)_3]_2[\alpha\text{-}SiW_{12}O_{40}]$,[178] which has a flexible structure composed of 2D-layers of polyoxometalates $[\alpha\text{-}SiW_{12}O_{40}]^{4-}$, macrocations $[Cr_3O(OOCC_2H_5)_6(H_2O)_3]^+$, and Ag^+ ions. This material can selectively adsorb small unsaturated hydrocarbons such as ethylene, propylene, *n*-butene, acetylene, and methyl acetylene over paraffins and larger unsaturated hydrocarbons. The sorption ratios of ethylene/ethane and propylene/propane are over 100 at 298 K and 100 kPa. Detailed research demonstrated that this selectivity can be attributed to the π-complexation with Ag^+ of small unsaturated hydrocarbons.

4.4 Selective adsorption based on adsorbate-specific gate-opening pressures

Different from all of the aforementioned adsorption characteristics, the phenomenon of guest adsorbates being permitted to pass through the gate at a specific gate-opening pressure, depending on the strength of the intermolecular interaction, has been observed in at least three flexible/dynamic MOFs. For such a flexible MOF, each gas has its own gate-opening pressure. Below this pressure, the gas molecules cannot be adsorbed. Several types of gases may thus be separated at different pressures by just one adsorbent. The first example is $Cu(dhbc)_2(4,4'\text{-bpy})$,[158] which in its hydrated form has a 2D sheet motif (Fig. 13). The sheets have interlocking ridges and hollows furnished by the dhbc benzene planes in an upright fashion and are mutually interdigitated to create 1D channels with a cross section of 3.6 × 4.2 Å, in which water molecules are accommodated. In addition, there exist interlayer π···π stacking interactions between neighboring dhbc ligands, which stabilize the 3D stacking structure. The N_2, O_2, CO_2, and CH_4 adsorption isotherms showed initially a flat curve indicative of zero adsorption in the low pressure

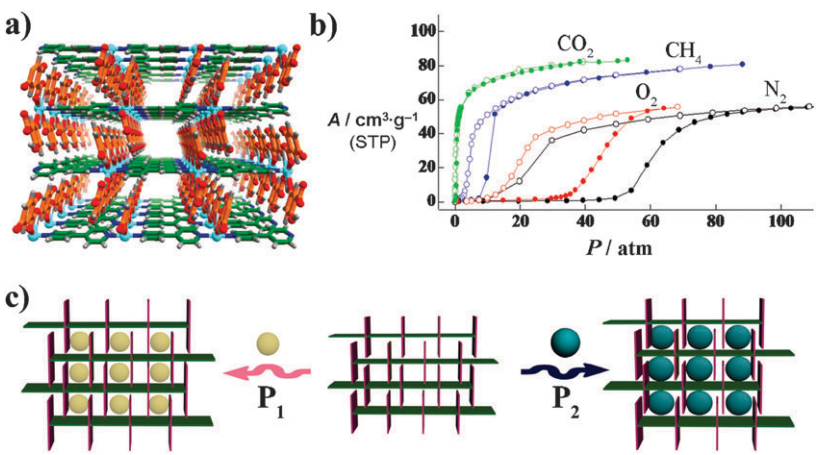

Fig. 13 (a) 3D π-stacked pillared layer structure of $Cu(dhbc)_2(4,4'\text{-bpy})$. (b) Gas adsorption (filled circles) and desorption (open circles) isotherms at 298 K. (c) Schematic representation of the gas selective adsorptions in the dynamic framework $Cu(dhbc)_2(4,4'\text{-bpy})$ whose gap open size depends on the guest molecules at special pressures.[158]

region, followed by an abrupt increase at a specific gate-opening pressure in each case. For each gas, the adsorption isotherm showed an abrupt decrease at another pressure, the gate-closing pressure, leading to a hysteresis loop of sorption. Interestingly, each gas has its distinct gate-opening and gate-closing pressure, which is related to differences in the intermolecular interaction force of the gas molecules. Additional flexible MOFs similar to $Cu(dhbc)_2(4,4'\text{-bpy})$ are Cu(pyrdc)(bpp)[163] and Cd(bpndc)(4,4′-bpy).[173] The former has a 2D pillared-bilayer structure with channels and showed sponge-like dynamic behavior along with bond breaking and formation triggered by guest removal and inclusion. The selective gate-opening phenomenon observed in adsorbates such as CO_2, MeOH, and EtOH was accounted for by their H-bonding interactions with the framework host, *i.e.*, such guests were allowed to pass through the gate at distinct gate-opening pressures depending on their strengths of H-bonding with the framework host. The latter has a structure similar to that of $Cu(dhbc)_2(4,4'\text{-bpy})$;[158] 2D layers are mutually interdigitated to create a 3D framework with 1D channels. Adsorption experiments of O_2, N_2, and Ar showed abrupt changes in its adsorption isotherms at the gate-opening pressures. It has been further demonstrated that the kinetics of the gate-opening process provides large differences in the onset pressures for different gas molecules, which can be selectively adsorbed at different pressures.

In summary, although the rearrangement mechanism of flexible frameworks is not completely clear, the flexible and dynamic framework of these MOFs provides a unique opportunity in exploiting new materials for specific applications. In the design and synthesis, combining both strong bonds and weak intermolecular interactions into a MOF entity is ideal for creating a flexible, dynamic MOF. The strong bonds ensure the integrity and porosity of the framework while the weak interactions allow certain flexibility. So far, for the majority of the flexible MOFs, the single-crystal structural analyses were limited to the solvated forms. There is still much unknown concerning the structure of the de-solvated MOFs. Further in-depth investigations will provide new insights and novel properties. In adsorptive separation, these soft materials are expected to exhibit more unusual behaviors in addition to their dynamic features. These unique properties will provide special applications in separation-related industries, such as the multilevel separation (step-by-step processes) of a mixture containing more than two components by using only one adsorbent at different temperatures and/or pressures.

5. Selective gas adsorption in mesh-adjustable metal–organic framework molecular sieves

Inorganic zeolite molecular sieves are currently the most used industrial adsorbents for gas separation. The rigidity of the bonds in zeolites usually affords them fixed mesh sizes. This is beneficial when the mesh size precisely fits the separation needs. However, when the size disparity of the two gases is very small, a zeolite molecular sieve with the precise mesh size is not always readily available. In such cases, mesh-adjustable molecular sieves (MAMSs) that can always meet the separation needs are highly desirable. Indeed, the mesh modulation of a molecular sieve material to a very limited range has been achieved in a few zeolites. For example, the titanosilicate molecular sieve ETS-4 can be systematically contracted through dehydration at elevated temperatures to tune the effective size of the pores, thereby tailoring the adsorption properties of this material to give size selective adsorbents suitable for separations of gas mixtures with close sizes.[155] Another example is the adsorption of O_2, Ar, and N_2 on zeolite A. At lower temperatures, N_2 and Ar do not diffuse into zeolite A, yet with increasing temperature, the size of the aperture increases enough to permit the diffusion of N_2 and Ar.[179] Additionally, NH_3 can enter the A cage of sodalite but not the B cage at low temperature, yet at high temperature both A and B can be filled.[180]

Recently, we reported the first MOF-based mesh-adjustable molecular sieve, MAMS-1, which was constructed from the amphiphilic ligand 5-*tert*-butyl-1,3-benzenedicarboxylate (bbdc) and Ni^{II} cluster.[181] MAMS-1 has a layer structure, consisting of hydrophilic channels and hydrophobic chambers, which are interconnected with each other through a size-adjustable gate (Fig. 14a). Variable temperature gas adsorption studies on activated MAMS-1 revealed that it exhibits a temperature-dependent selective gas adsorption effect (Table 7), and its gate size range falls between about 2.9 and 5.0 Å. Indeed, there exists a linear relationship between the gate size and temperature, $D = D_0 + \alpha T$ (D: mesh size at T K, D_0: mesh size at 0 K, and α: a constant). When the temperature is precisely controlled, any size within this range can be accurately attained. Commercially relevant gas separations, such as those of H_2/N_2, H_2/CO, N_2/O_2, N_2/CH_4, CH_4/C_2H_4, and C_2H_4/C_3H_6, may thus be achieved by MAMS-1. Primary mechanism analyses suggested that the hydrophobic chambers are the major storage room for gas molecules, yet the gas has to first pass through the fully activated hydrophilic channels to enter the hydrophobic chambers. Pairs of bbdc ligands at the interface of hydrophilic channels and hydrophobic chambers serve as the gate, which opens linearly with increasing temperatures allowing gas molecules with the appropriate sizes to enter the hydrophobic chambers (Fig. 14b). This remarkable result showed that it is possible to design a temperature-swing apparatus based on MAMS-1 to perform fractional adsorption to separate a multi-component gas mixture. Our ongoing work is being focused on systematically tuning the ligands and/or metal clusters to tailor the adsorption properties of MAMSs to make gas separations feasible at ambient temperatures and applicable pressures.[182] Furthermore, the temperature-triggered gate opening phenomenon has also been observed recently in the microporous MOFs $Mn(HCOO)_2$[149] and Cu(etz).[175]

It must be pointed out that most of the selective gas adsorption studies in MOFs were focused on adsorption isotherm measurements of single-component gases reflecting primarily the adsorption equilibrium of one component. Based on these adsorption isotherms alone, the kinetic effect, which is critical in practical gas separation, cannot be evaluated. In fact, equilibrium adsorption is not adequate to predict selectivity, because dynamic capacity is strongly influenced by the adsorption kinetics. Until now, only one report was

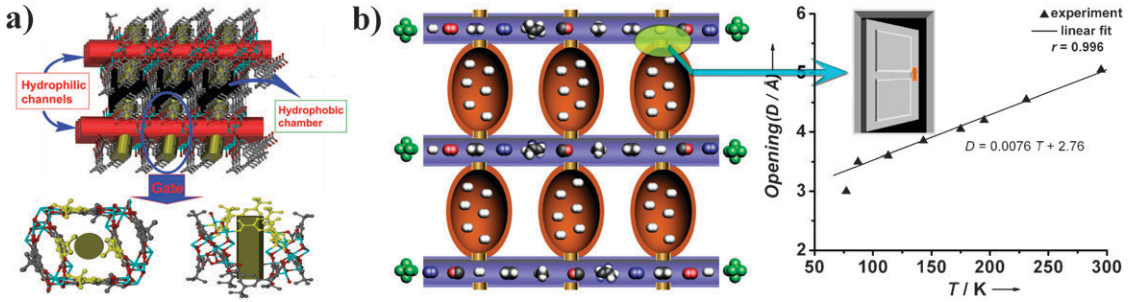

Fig. 14 (a) Structure of MAMS-1. (b) Schematic representation of selective gas adsorption and temperature-dependent gate opening in MAMS-1.[181]

Table 7 Selective gas adsorption data of MAMS-1[a]

T/K	Adsorption Selectivity	Uptake (at 1 P/P°)
77	H_2 over CO, O_2, and N_2	H_2, 3.7 mmol g^{-1}; CO, O_2, and N_2, almost none
87	O_2 over CO and N_2	O_2, 4.3 mmol g^{-1}; CO and N_2, <1 mmol g^{-1}
113	N_2 over CO and CH_4	N_2, 2.4 mmol g^{-1}; CO and CH_4, <0.7 mmol g^{-1}
143	CH_4 over C_2H_4	CH_4, 3.2 mmol g^{-1}; C_2H_4, <0.8 mmol g^{-1}
195	C_2H_4 over C_3H_6	C_2H_4, 3.1 mmol g^{-1}; C_3H_6, <1 mmol g^{-1}
241	C_3H_6 over *iso*-C_4H_{10}	C_3H_6, 3.6 mmol g^{-1}; *iso*-C_4H_{10}, <0.8 mmol g^{-1}

[a] All data was obtained directly from the original literature.

documented in the study of dynamic gas adsorption properties for MOFs, in which the dynamic adsorption capacity of several MOFs for harmful gases: SO_2, NH_3, Cl_2, CO, C_6H_6, CH_2Cl_2, C_2H_4O (ethylene oxide), and C_4H_8S (tetrahydrothiophene) have been evaluated by kinetic breakthrough measurements.[68] The results showed that the adsorption capacity of such MOFs is comparable to (or even better than) that of BPL activated carbon and that the pore functionality plays an important role in determining the dynamic adsorption performance of MOFs for these gases and vapors. In addition, gas adsorption studies using a mixture of gases has been reported in only a few cases.

6. Molecular simulations of adsorptive gas separation in metal–organic frameworks

With the ever-growing computational power, molecular simulations have been playing an increasingly important role in the various fields of science and technology.[183] In the field of adsorptive gas separation, the molecular simulation is an ideal tool to screen existing adsorbents for a given separation task. Due to the predictability of the syntheses of some materials, such as metal–organic frameworks (to some extent), simulations also offer the possibility to test hypothetical materials. In addition, at the molecular level, a theoretical simulation might help to explain the macroscopic phenomena of adsorption and separation. The studies of adsorptive gas separation with metal–organic frameworks contain simulations not only in adsorption equilibria but also in diffusion dynamics from a single component to a gas mixture.

6.1 Molecular simulations of selective gas adsorption and separation in metal–organic frameworks

Most of the experimental studies on selective gas adsorption in MOFs are based on isotherm measurements of single component adsorbate; studies dealing with mixed adsorbates molecules and addressing the potential use in separations are still rare. However, molecular simulations have been commonly performed on the adsorption and separation of mixture gases in some representative MOFs such as MOF-5 [$Zn_4O(bdc)_3$], HKUST-1 [$Cu_3(btc)_2$], and a few other isoreticular MOFs (IRMOFs).

On MOF-5, the simulation of the adsorption and separation of linear and branched alkanes at 300 K showed that competitive adsorption occurs as a result of size and/or configuration differences.[184] For a mixture of C1 to C5 linear alkanes, the adsorption of long-chain alkanes increases first and decreases with increasing fugacity, whereas short-chain alkanes adsorption increases continuously and gradually replaces the long-chain alkanes at high fugacity. For a three-component mixture of C5 isomers, the linear isomer has a greater adsorption uptake than that of branched ones. The uptake of *n*C5 and *i*C5 relative to that of *neo*C5 increases first with increasing fugacity and decreases to a constant near saturation. The studies of the absorption selectivity for C4 ~ C6 alkane isomer mixtures in MOF-5 and IRMOF-6 revealed that the selectivity is mainly controlled by the adsorption enthalpy when the alkane mixtures are adsorbed in the pore channels, but by the adsorption entropy when they are close to the Zn_4O cluster.[185] The studies also confirmed that the separation capability of IRMOF-6 is higher than that of MOF-5. Furthermore, the CH_4/*n*-C_4H_{10} adsorptions and separations in MOF-5, 8, 10, 14, and 16 at 298 K have been assessed.[186] The results showed that *n*-C_4H_{10} molecules tend to locate in the corners of the MOF cavities whereas the CH_4 molecules occupy the center of the cavity. The adsorption selectivity for *n*-C_4H_{10} over CH_4 increases with decreasing pore size and an increasing number of C atoms in the organic linkers. At 10 kPa, the selectivity (75 ~ 280) in MOF-5 decreases with increasing bulk mole fraction, whereas the selectivity in the other materials is nearly constant. However, at 100 kPa, this situation occurs in almost all materials (except MOF-16), and their selectivity is large (50 ~ 250) and exhibits a sudden drop for smaller mole fractions of *n*-C_4H_{10}. These estimated selectivities are as good as or better than experimentally observed selectivities in other

porous adsorbents. In addition, it has been recently demonstrated that the selective adsorption of CH_4 over H_2 is enhanced in the interpenetrated IRMOFs compared to their non-interpenetrated counterparts, and CH_4 selectivity is more complicated in the former and the selectivity differs significantly in different areas of the pores.[187] This has been attributed to the existence of various small pores with different sizes in the framework brought on by the interpenetration.

In the studies of HKUST-1, the research on C_2H_4 and C_2H_6 adsorptions showed that at low loadings C_2H_4 has a higher binding energy, which leads to the selective adsorption of C_2H_4 by a factor of about two at low pressure.[188] However, at high loadings the selectivity is not obvious. This indicates that the adsorbate–pore surface interactions can lead to selective adsorption of light hydrocarbons at low pressure. A systematic evaluation of the adsorptive separation of CO_2/CO, C_2H_4/CO_2, and C_2H_4/C_2H_6 in HKUST-1 at 298 K has also been performed by molecular simulations.[189] The results indicated that with equimolar composition, the selectivity for CO_2 from CO_2/CO increases (from 10 to 23) gradually at first and then becomes nearly independent of the pressure; for C_2H_4 from C_2H_4/CO_2 the selectivity decreases quickly with loading at low pressure and then becomes independent of the pressure giving a value of 1; for C_2H_4 from C_2H_4/C_2H_6 the selectivity initially decreases at low pressures and then becomes independent of the pressure while increasing to two with the increase in pressure. The simulations of separation of CO_2 from flue gases (a mixture of $CO_2/N_2/O_2$) using HKUST-1 also showed that this material is promising for separating CO_2 from flue gases, and the temperature and gas composition are important in optimizing the separation process.[190] It has been realized that the local structure of the side pockets in HK UST-1 framework is responsible for the selective adsorption behaviors, especially at low adsorption loadings. Furthermore, it has been demonstrated that the electrostatic field inside the pores of HKUST-1 is especially important for the selective adsorption of polar (such as CO) and quadrupolar (such as CO_2) molecules,[188,190,191] some of which have also been confirmed in experiments. As a result, this MOF adsorbent may be effective for the purification and capture of CO_2 or CO, and olefin/paraffin separation.

In addition, a systematic computational study of the purification of synthetic gas by MOF-5 and HKUST-1 has also been performed.[192] The results showed that MOF-5 has simple selectivity behaviors, but HKUST-1 resulted in complex selectivity behaviors with different selectivity steps, and in each case both pore size and geometry have great influences on the separation efficiency. With an equimolar adsorbate mixture, MOF-5 and HKUST-1 exhibit the selectivity of CO_2 over CH_4 of $2\sim3$ and $6\sim9$, CH_4 over H_2 of $5\sim6$ and $10\sim18$, and CO_2 over H_2 of $10\sim35$ and $80\sim150$, respectively at 298 K. Furthermore, it was confirmed that the electrostatic interactions between adsorbed molecules and host frameworks can greatly enhance the separation efficiency of gas mixtures. This effect has also been reported in a similar investigation on the adsorption of CO_2, CH_4, C_2H_6, and their mixtures in HKUST-1.[193]

Most recently, by molecular simulations, another MOF, $Zn_2(bdc)_2(dabco)$ (dabco represents 1,4-diazabicyclo[2.2.2]-octane), has been demonstrated to be highly promising for separating alkanes based on the degree of branching in a multi-component mixture (13-component), which may become valuable for removing low RON alkanes from a mixed stream.[194]

6.2 Molecular simulations of gas diffusion in metal–organic frameworks

In adsorptive separation the diffusivity of the gas molecules into the porous material is of crucial importance. Experimental information on the diffusion of gases in MOFs is, however, still scarce.[195,196] Compared to zeolites, the theoretical studies for gas diffusion in MOFs are also not extensive, and most of them are focused only on single component gas systems. The diffusivities, including self-diffusivity and transport diffusivity, can be calculated by using equilibrium molecular dynamics (EMD) and/or grand canonical Monte Carlo (GCMC) simulations. For the first time, gas diffusion in HKUST-1 has been studied by Skoulidas by using molecular dynamic (MD) simulations.[197] The results showed that the transport diffusivity of Ar in HKUST-1 at room temperature differs from the self-diffusivity by about 2 orders of magnitude at high loadings. Indeed, this diffusion is very similar to that in silica zeolites in magnitude, concentration, and temperature dependence. In addition, the self-diffusion and transport diffusion of Ar, CH_4, CO_2, and N_2 in MOF-5 (IRMOF-1), and Ar diffusion in three other IRMOFs have also been investigated using molecular simulations.[198] For Ar, CH_4, and N_2, the concentration dependence is simple, and the transport diffusivity increases monotonically as the pore loading increases in MOF-5. However, for CO_2 the transport diffusivity is a nonmonotonic function of pore loading. At zero loading, the order of the self-diffusivities is $H_2 > N_2 \approx CH_4 \approx Ar > CO_2$, and the self-diffusivity decreases with increasing concentration for each gas. Moreover, at zero loading the diffusivities of Ar in all these materials span less than an order of magnitude and the relative magnitude of the zero loading diffusivity is not correlated to the pore size of the MOFs. In addition, the self-diffusivities of *n*-C_5H_{12}, *n*-C_6H_{14}, *n*-C_7H_6 and *cyclo*-C_6H_{14} in MOF-5, which are of the same order of magnitude as in silicalite, have also been simulated.[199] For the *n*-alkanes a stronger dependence on chain length has been confirmed. Cyclohexane also diffuses on the MD time scale and the diffusivity is slightly higher than that of *n*-hexane.

For the simulations of gas mixture diffusion, only one report was documented.[200] In this work, the diffusion of CO_2, CH_4, and their mixture in MOF-5 using MD simulations was investigated. The results showed that as loading increases the self-diffusivities in this material decreases as a result of the steric hindrance, and the transport diffusivities increase for CH_4 but are nonmonotonic for CO_2. In the CO_2/CH_4 binary mixture, the self-diffusivities for both components decrease with increased loading. As the loading rises, the permselectivity slightly increases with an overall value close to unity.

The aforementioned theoretical investigations using molecular simulations have confirmed that MOFs are promising candidates as new adsorbents for gas separation and purification. Such results will direct the research to further exploit the separation applications of this new class of materials.

However, all of the simulations mainly focus on several typical MOFs, such as MOF-5 and HKUST-1; further work is required for other MOFs due to their structural diversity and compositional complexity. For flexible/dynamic MOFs, molecular simulations may be useful not only in adsorptive gas separation but also in structural comprehension of their adsorbed/desorbed forms. In conclusion, molecular simulations will play an important role in the on-going development of MOFs and their applications in gas separation.

7. Gas separation with metal–organic frameworks

Selective adsorption characterizations and molecular simulations have demonstrated that MOFs have great potential in the separation and purification of gas or vapor mixtures. However, investigations in actual separations of gas mixtures with MOFs are scarce, although recent studies in kinetic separation, isotope separation, and membrane-based separation have illustrated an encouraging potential for real applications. It should be noted that under a given temperature and pressure some MOFs possess gas adsorption selectivity due to the molecular sieving effect. In principle, these MOFs can separate a gas mixture containing multiple components at conditions similar to that of the adsorption of a single component. The next step is the design of a process to perform the separation based on molecular sieving. However, in some other MOFs the pores are well-situated or large enough to accommodate several types of gases yet still exhibit adsorption selectivity arising from thermodynamic equilibrium or the kinetic effect. In this instance, a kinetic separation experiment is very helpful in further evaluating the separation ability.

7.1 Kinetic separation in metal–organic frameworks

Different from the molecular-sieving effect, kinetic separation is accomplished by virtue of the differences in the diffusion rates of different components. This is of great importance in industrial applications, particularly in chromatography applications. Diffusion rates are determined by the relationship between the adsorbate molecule's size and shape and the size and shape of the adsorbent's pore, the strength of adsorption, the affinity to adsorption sites, the concentration of adsorbed species, the system temperature, and so on. Kinetic separation is usually characterized by a time-dependent adsorption or the discharging of different adsorbate components. The procedures include gas-chromatographic separation, fixed-bed adsorption, and other methods, which usually give a breakthrough curve. For the first time, Wang *et al.*[106] have studied gas separation and purification by HKUST-1 through thermodynamic and breakthrough experiments and demonstrated that it can be used for the separation of gas mixtures such as CO_2/CO, CO_2/MeOH, and C_2H_4/C_2H_6 mixtures. In addition, this research also showed that air can be purified effectively from CO_2, NO, high-molecular weight hydrocarbons, and moisture by using this material. Similar investigations have been performed for the separation of CF_4 and Ar by $Co_3(bpdc)_3(bpy)$ and HKUST-1.[201] HKUST-1 prepared by using different routes was also tested for adsorptive separation of isobutene and isobutane.[202] The results showed that more isobutene was adsorbed than isobutane at different temperatures. However, the difference in adsorption capacity cannot solely be attributed to the strong interaction between the Cu centers and isobutene due to only small difference in enthalpies of adsorption. The breakthrough experiments revealed the separation with a factor of 2.1 can be achieved and that a low pressure separation is preferred in this case.

The separation of mixed C_8 alkylaromatic compounds (*p*-xylene, *o*-xylene, *m*-xylene, and ethylbenzene) is one of the most challenging issues in the chemical industry due to the similarity of their boiling points and dimensions.[203] This separation is currently performed by cation-exchanged zeolites X and Y in industry, yet adsorbents with improved separation efficiency are still needed. Recently, Alaerts *et al.*[204] investigated the adsorption and separation of a mixture of C_8 alkylaromatic compounds in the liquid phase using three MOFs: HKUST-1, MIL-47, and MIL-53(Al). Chromatographic experiments demonstrated that MIL-47 has the highest potential for real separations of C_8 alkylaromatic compounds among the three investigated MOFs. They also studied the pore-filling-dependent selective effects in the C8 alkylaromatic vapor separation on MIL-47.[205] Adsorption and breakthrough experiments showed that the separation of these isomers could be achieved accurately by using this MOF, and that the adsorption selectivity increases with increasing partial pressure or degree of filling. It was also confirmed that the separation at a high degree of pore filling is a result of differences in packing modes of such components in the pores. Thus, the adsorption selectivity seems to be strongly dependent on pressure and temperature, which are powerful tools in the optimization of the separation process. In addition, MIL-53(Al) was further tested for the selective adsorption and separation of xylenes, ethylbenzene, ethyltoluenes, and cymenes by using batch, pulse chromatographic, and breakthrough experiments.[206] The results indicated that this MOF has the largest affinity for the *ortho*-isomer among the alkylaromatic compounds, and the *ortho*-compounds can be separated from other isomers using a column packed with MIL-53(Al). It was also demonstrated that for xylenes molecular packing plays an important role, and the interactions of methyl groups of the xylenes with the pore walls of MIL-53(Al) determine selectivity. Compared to MIL-47, the adsorption preferences for alkylaromatics found on MIL-53(Al) are different. MIL-53(Al) is more effective in the separation of ethyltoluene and cymene isomers than MIL-47.

The separation of hexane isomers to boost octane ratings in gasoline is a very important process in the petroleum industry.[207] This is still achieved by using the high-energy-consuming method of cryogenic distillation. By making use of the pore to capture and discriminate hexane isomers, MOFs have the potential to separate them. This was well illustrated by Bárcia *et al.*[208] in the kinetic separation of hexane isomers by using a 3D microporous MOF, $Zn_2(bdc)_2(dabco)$. This MOF contains 3D intersecting pores of about 7.5 × 7.5 Å in one direction and pores of 3.8 × 4.7 Å in the other two directions. By using the narrow channels to exclusively take up linear *n*-hexane while blocking branched hexane isomers, this MOF was successfully used in the kinetic separation of hexane isomers by fixed-bed adsorption. It exhibits the extraordinary ability to separate branched hexane

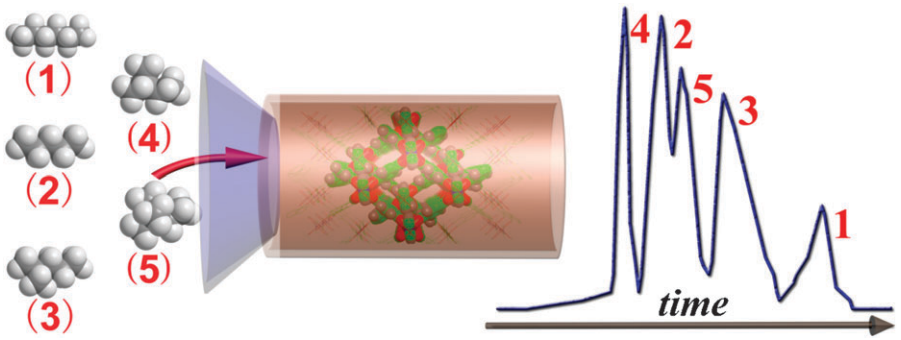

Fig. 15 Schematic representation of the GC separation of alkanes with MOF-508 (*n*-hexane (1), *n*-pentane (2), 2-methylpentane (3), 2-methylbutane (4) and 2,2-dimethylbutane (5)).[210]

isomers from linear *n*-hexane. As the first example, this result demonstrated the great potential of MOFs for applications in the very important industrial process of hexane-isomers separation.

The process for enhancing octane ratings in gasoline also includes the separation of other alkane isomers, which is currently carried out by using zeolites.[209] A microporous MOF, MOF-508 has been demonstrated to be useful in the gas-chromatographic (GC) separation of alkanes in Chen's group.[210] Fig. 15 schematically presents the GC separation of alkane mixtures with this MOF. MOF-508 has an interpenetrated 3D pillared-layer structure with 1D open channels, which can selectively adsorb linear alkanes and discriminate branched ones. This material was also confirmed to be able to efficiently separate natural gas mixtures by a GC method. It was suggested that the subtle matching of the size and shape of the alkanes with the micropores of MOF-508 leads to different van der Waals interactions, resulting in the adsorptive separation of alkanes in the MOF-508 column.[211]

It is believed that CO_2 emissions lead to the deterioration of the earth's environment. The efficient and selective capture of CO_2 from industrial emission streams is still a challenging task.[212,213] In addition, the removal of CO_2 from CH_4 is very important for CH_4 transportation and usage, as well as for preventing the corrosion of equipment and pipelines. ZIFs recently developed by Yaghi's lab[140,141] seem to be capable of solving these problems. Such porous MOFs have good stability and a unique framework structure composed of large cages connected by small windows. Large cages have a high capacity for accommodating guest molecules, and the small windows can limit some molecules from entering the cages. Indeed, several ZIFs have been confirmed to have the ability to selectively capture and store CO_2. For example, adsorption isotherms showed that ZIF-95 and ZIF-100 have a high capacity for the adsorption of CO_2 at 298 K but not for CH_4, CO, and N_2. Preliminary breakthrough experiments showed that CO_2 can be held in the pores of ZIF-95 and ZIF-100 when exposed to streams containing binary mixtures of CO_2/CH_4, CO_2/CO, or CO_2/N_2 (50:50 v/v). Similarly, ZIF-68, ZIF-69, and ZIF-70 can separate CO_2 from a CO_2/CO mixture, which have also been confirmed by breakthrough experiments. The selectivities of these ZIFs for CO_2 are higher than those of other porous materials. In addition, $Zn(bdc)(4,4'\text{-bipy})_{0.5}$ has also been examined for the separation and removal of CO_2 from its binary CO_2/N_2, CO_2/CH_4, and ternary $CO_2/CH_4/N_2$ mixtures by fixed-bed adsorption.[214] Both breakthrough curves and adsorption isotherms indicated that this MOF is also efficient in the removal of CO_2. In the adsorption isotherms of binary and ternary mixtures, the amount of the adsorbed components is inversely proportional to the temperature but directly proportional to the partial pressure, the same as was seen for single component adsorption. However, the CO_2 uptake is much more temperature-dependent than either N_2 or CH_4, causing the selectivity for CO_2 to increase with an increase in partial pressure and a decrease of temperature.

In addition, the separation of noble gases is very important in industry and medical fields. For instance, Kr is applied as a filler in the lamp industry, and Xe can be used as a narcotic medicinal gas. Such gases are usually obtained by separating air using cryogenic technology. Recently, scientists from BASF have demonstrated that a simple process of pressure-swing adsorption is feasible in the separation of noble gases by using HKUST-1 as an adsorbent.[36] The experimental results showed that HKUST-1 can effectively separate Xe and Kr by continuous adsorption. The former was adsorbed easily, while the later was adsorbed to a much lesser extent. The calculated capacity of HKUST-1 for Xe is more than 60 wt%, almost twice as much Xe as that on a high-surface-area active carbon.

7.2 Quantum sieving effect for H_2/D_2 separation by metal–organic frameworks

The classical sieving principle of molecular sieves cannot be applied to isotope separation because isotopic molecules have identical adsorption-based properties. In contrast, a quantum molecular sieving process is applicable for isotope separation, which was proposed by Beenakker *et al.*[27] Quantum sieving is based on the preferential adsorption of heavier isotopes due to the difference in the quantum energy levels of atoms or molecules confined in a very narrow space that is comparable to the de Broglie wave length. This effect has been demonstrated for H_2 and D_2 separation in single wall carbon nanohorns,[215] porous carbon materials,[216] zeolites,[217] and activated carbon fibers,[218] with both adsorption equilibria and/or kinetics. Recently, the quantum sieving effect of MOFs for H_2 and D_2 has also been observed in

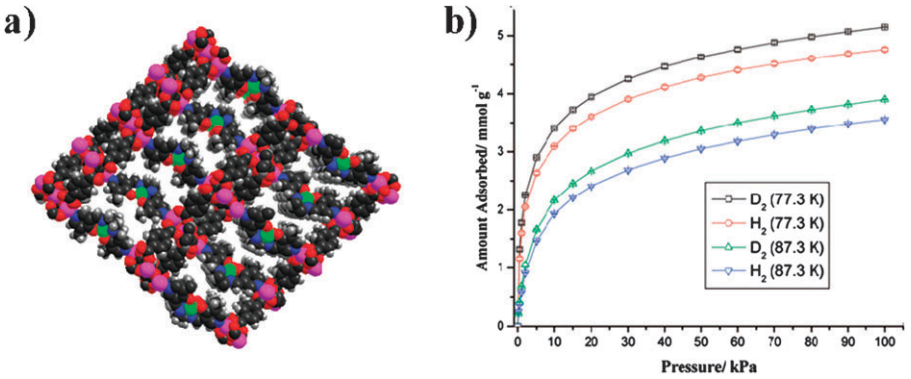

Fig. 16 (a) Structure of $Zn_3(bdc)_3[Cu(Pyen)]$ showing curved micropores. (b) Adsorption isotherms of $Zn_3(bdc)_3[Cu(Pyen)]$ for H_2 and D_2.[219]

$Zn_3(bdc)_3[Cu(Pyen)]$[219] ($PyenH_2$ = 5-methyl-4-oxo-1,4-dihydropyridine-3-carbaldehyde) and $[Cu(4,4'\text{-bipy})_2(CF_3SO_3)_2]$.[220] $Zn_3(bdc)_3[Cu(Pyen)]$ contains a gridding $Zn_3(bdc)_3$ 2D layer that is pillared by Cu(Pyen) to form a 3D structure containing approximately a 2D array of pores, with larger pores of about 5.6 × 12.0 Å in the crystallographic *c* direction and irregular ultramicropores in the *b* direction (Fig. 16a). The investigations indicated that the adsorption of H_2 and D_2 occurs on both sides of the open Cu^{II} centers in ultramicropores and affords a very high enthalpy of adsorption. Both adsorption equilibria (Fig. 16b) and kinetics studies demonstrated that the quantum effects of H_2 and D_2 adsorption and separation occur in this MOF. This effect influences the diffusion of H_2 and D_2 into pores. The virial analysis of isotherm data also demonstrated slightly greater D_2-surface than H_2-surface interactions, which can be attributed to differences in the quantum statistical mass effect on the vibrational energy levels of two gases. In the adsorption kinetics, the rate constants for D_2 are larger and the activation energies slightly lower than the corresponding values for H_2. This was ascribed to the quantum effect with the higher zero-point energy of H_2 affording a more effective collision cross section than D_2, which produces a higher barrier to diffusion in the pores. $[Cu(4,4'\text{-bipy})_2(CF_3SO_3)_2]$ has a 3D structure with two types of 1D channels having different sizes (8.7 and 2.0 Å). Similarly, adsorption experiments and molecular simulations showed that this MOF holds great potential in quantum sieving separation of H_2 and D_2. In view of the diversity of MOFs, more efforts should be devoted to both the exploration of existing MOFs and the design and synthesis of new MOFs for quantum sieving separation.

7.3 Membrane-based gas separation with metal–organic frameworks

Membrane-based gas separations have been widely used in industry and have demonstrated operational advantages over other separation approaches, especially in large-scale applications.[221] The efficiency of this technology depends mainly on the selection of the membrane materials, their properties, and the permeation mechanism. Polymeric membranes are widely available but possess a fundamental trade-off between selectivity and throughput. Thin films of crystalline porous materials have great potential for avoiding this tradeoff, but the selection of the membrane materials is a challenge.[222] MOFs, as newly developed porous materials, are also promising membrane materials, although only one example of a MOF thin film for gas separation has been recently reported: a copper net supported $Cu_3(btc)_2$ MOF film (Fig. 17).[223] This thin film was successfully prepared by means of a "twin copper source" technique using an oxidized copper net to provide homogeneous nucleation sites for the continuous crystal film growth in the solution containing Cu^{2+} ions and organic ligand H_3btc. The results of membrane-based separation of H_2/N_2, H_2/CO_2, and H_2/CH_4 mixtures showed this MOF film has a high H_2 permeation flux (0.107 mol m^{-2} s^{-1}, being larger than its partners) and an

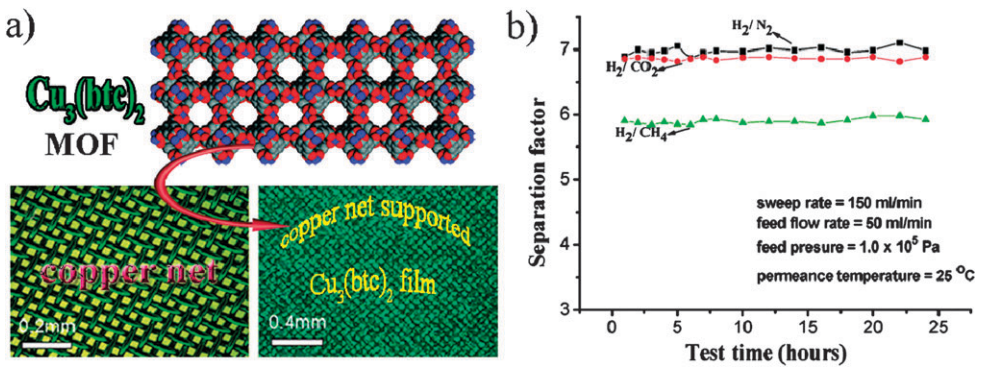

Fig. 17 (a) Structure of $Cu_3(btc)_2$ MOF and optic micrographs of the copper net and copper net supported $Cu_3(btc)_2$ membrane. (b) Plot of H_2/N_2, H_2/CH_4, and H_2/CO_2 separation factor of the copper net supported $Cu_3(btc)_2$ membrane with change in test time.[223]

excellent permeation selectivity for H_2 with the separation factor being 7.04, 6.84, and 5.92, respectively (298 K, 1 atm with a 1 : 1 volume ratio gas mixture). The permeability and selectivity of this MOF-based membrane are better than those of conventional zeolite membranes. More so, it also has good stability and recyclability, thus being suitable for applications in separating or purifying H_2. In addition, recent theoretical simulations also demonstrated that MOFs may be feasible as membrane materials for gas separation.[224] In this work atomistic simulations were used to assess the separation of CO_2/CH_4 mixtures by a MOF-5 membrane. The single-component permeation results predicted that MOF-5 membranes would show strong selectivity for CH_4 in CO_2/CH_4 mixtures whereas the predictions for mixture permeation suggested that this membrane will offer only weak selectivity for CO_2.

On the other hand, hybrid membranes or mixed matrix membranes are another option for the application of MOFs in membrane-based separation. This concept involves the incorporation of MOFs within a polymeric matrix, resulting in a hybrid membrane material with superior selectivity. However, the explorations are very limited with only few reports. Won *et al.*[225] have prepared a molecular sieve composite membrane by using molecular dispersions of a 3D MOF, $[Cu_2(PF_6)(NO_3)(4,4'\text{-bpy})_4]\cdot 2PF_6\cdot 2H_2O$, confined in polysulfone (PSf). The separation of He, H_2, O_2, N_2, and CH_4 gases with this membrane showed it has enhanced selectivity for H_2 and He over CH_4 at 5 wt% MOF loading. Car *et al.*[226] investigated the separation of H_2, O_2, N_2, CO_2, and CH_4 by two MOFs, HKUST-1 and $Mn(HCOO)_2$ in polydimethylsiloxane (PDMS) and PSf polymer matrices. The results indicated that the gas separation ability of these hybrid membranes has been improved in permeability for H_2, CO_2, and CH_4, as well as in selectivity for H_2 over N_2 and CO_2 over N_2, when compared to pure polymeric membranes. In addition, mixed-matrix membranes of Matrimid® containing MOF-5 for gas separations (H_2/CO_2, CH_4/CO_2, and CH_4/N_2) have also been investigated by Perez *et al.*[227] The results showed that the ideal selectivity of these mixed membranes for any gas pairs did not increase compared to Matrimid®, but the permeabilities increased 120% at 30% MOF-5 loading. Gas mixture separation tests showed an obvious increase in selectivity for CH_4 but remained constant for H_2 under all gas feed conditions. Taking advantage of the tunable pore size, modifiable pore surface, and adjustable structure, MOFs will have a truly bright future in membrane-based separation.

8. Conclusion

Environmentally benign and cost-effective gas separation represents one of the most urgent needs in our society today. In adsorptive separation, the exploitation of new adsorbents is critical yet very difficult because of the many requirements posed by industry and environmental protection. As potential adsorbents, MOFs have attracted a great deal of interest. The progress that has been made in this important field is evident: from single-component gas adsorption to the separation of a multi-component mixture, from the molecular sieving effect to the kinetic effect, from pressure swing to temperature swing operation, from gas-chromatographic separation to fix-bed adsorption, from adsorption-based separation to membrane-based separation, from clean energy-related gases to harmful gases, from noble gases to isotopes, and from experimental work to molecular simulations. However, we may have seen just the tip of the iceberg with respect to the application potential of MOFs in selective gas adsorption and separation.

Acknowledgements

This work was supported by the US Department of Energy (DE-FC36-07GO17033), the US Defense Logistics Agency (N00164-07-P-1300), and the US National Science Foundation (CHE-0449634). We thank Dr Da-Qiang Yuan for his helpful discussions and Prof. S. Kitagawa for providing high resolution figures.

References

1 C. J. King, *Separation Progress*, McGraw-Hill, New York, 2nd edn, 1980.
2 R. T. Yang, *Adsorbents: Fundamentals and Applications*, John Wiley & Sons, Hoboken, 2003.
3 B. L. Karger, R. L. Snyder and H. Horvath, *An Introduction to Separation Science*, Wiley, New York, 1973.
4 R. Xu, W. Pang, J. Yu, Q. Huo and J. Chen, *Chemistry of Zeolites and Related Porous Materials: Synthesis and Structure*, John Wiley & Sons (Asia) Pet Ltd., Singapore, 2007.
5 R. T. Yang, *Gas Separation by Adsorption Progress*, Butterworth, Boston, 1987.
6 F. Rouquerol, I. Rouquerol and K. Sing, *Adsorption by Powders and Porous Solids-Principles Methodology and Applications*, Academic Press, London, 1999.
7 C. W. Chi and W. P. Cummings, *Kirk-Othmer Encycl. Chem. Technol.*, John Wiley & Sons, New York, 3rd edn, 1978, vol. 1, p. 544.
8 F. Fajula and D. Plee, *Stud. Surf. Sci. Catal.*, 1994, **85**, 633–651.
9 G. V. Baron, *Process Technol. Proc.*, 1994, **11**, 201–220.
10 R. J. Allam, R. Bredesen and E. Drioli, *Carbon Dioxide Recovery Util.*, 2003, 53–120.
11 J. A. Ritter and A. D. Ebner, *Sep. Sci. Technol.*, 2007, **42**, 1123–1193.
12 T. Bein and S. Mintova, *Stud. Surf. Sci. Catal.*, 2005, **157**, 263–288.
13 F. G. Kerry, *Industrial Gas Handbook: Gas Separation and Purification*, CRC Press, Boca Raton, 2007.
14 T. E. Whyte, Jr, C. M. Yon and E. H. Wagener, *Industrial Gas Separation*, American Chemistry Society, Washington, DC, 1983.
15 S. M. Auerbach, K. A. Carrado and P. K. Dutta, *Handbook of Zeolite Science and Technology*, Marcel Dekker, Inc., New York, 2003.
16 J. Seader and M. Henley, *Separation Process Principles*, Wiley, New York, 1998.
17 D. D. Duong, *Adsorption Analysis: Equilibria and Kinetics*, Imperial College Press, London, 1998.
18 D. M. Ruthven, *Principles of Adsorption and Adsorption Processes*, John Wiley& Sons, New York, 1984.
19 A. Dabrowski, *Adv. Colloid Interface Sci.*, 2002, **93**, 135–224.
20 D. W. Beck, *Zeolite Molecular Sieves*, John Wiley & Sons, New York, 1974.
21 B. Crittenden and W. J. Thomas, *Adsorption Technology and Design*, Butterworth-Heinemann, Oxford, 1998.
22 P. A. Warrendale, *Nanoporous and Nanostructured Materials for Catalysis Sensor and Gas Separation Applications*, Materials Research Society, San Francisco, 2005.
23 J. M. Loureiro and M. T. Kartel, *Combined and Hybrid Adsorbents: Fundamentals and Applications*, Springer, Netherlands, 2006.
24 F. Schuth, K. S. W. Sing and J. Weitkamp, *Handbook of Porous Solids*, Wiley-VCH, New York, 2002.

25 P. A. Wright, *Microporous Framework Solids*, RSC Publishing, Cambridge, 2008.
26 J. U. Keller and R. Staudt, *Gas Adsorption Equilibria, Experimental Methods and Adsorptive Isotherms*, Springer Science+Business Media, Inc., Boston, 2005.
27 J. J. M. Beenakker, V. D. Borman and S. Y. Krylov, *Chem. Phys. Lett.*, 1995, **232**, 379–382.
28 M. Suzuki, *Adsorption Engineering*, Elsevier, Amsterdam, 1990.
29 E. N. Coker, D. P. Roelofsen, R. M. Barrer, J. C. Jansen and H. van Bekkum, *Microporous Mesoporous Mater.*, 1998, **22**, 261–268.
30 Y. Liu and R. L. Withers, *J. Solid State Chem.*, 2003, **172**, 431–437.
31 S. Sircar, *Ind. Eng. Chem. Res.*, 2006, **45**, 5435–5448.
32 S. Sircar and A. L. Myers, in *Gas Separation by Zeolites in Handbook of Zeolite Science and Technology*, ed. S. M. Aurbach, K. A. Carrado and P. K. Dutta, Dekker, New York, 2003.
33 B. E. Poling, J. M. Prausnitz and J. P. O'Connell, *The Properties of Gases and Liquids*, McGraw-Hill, New York, 5th edn, 2001.
34 D. R. Lide, *CRC Handbook of Chemistry and Physics*, CRC Press, 88th edn, 2007.
35 T. J. Barton, L. M. Bull, W. G. Klemperer, D. A. Loy, B. McEnaney, M. Misono, P. A. Monson, G. Pez, G. W. Scherer, J. C. Vartuli and O. M. Yaghi, *Chem. Mater.*, 1999, **11**, 2633–2656.
36 M. E. Davis, *Nature*, 2002, **417**, 813–821.
37 S. Kaskel, *Handbook of Porous Solids*, Wiley-VCH, New York, 2002, vol. 2, pp. 1190–1249.
38 A. Stein, *Adv. Mater.*, 2003, **15**, 763–775.
39 C. Sanchez, B. Julián, P. Belleville and M. Popall, *J. Mater. Chem.*, 2005, **15**, 3559–3592.
40 D. Bradshaw, J. B. Claridge, E. J. Cussen, T. J. Prior and M. J. Rosseinsky, *Acc. Chem. Res.*, 2005, **38**, 273–282.
41 J. Yu and R. Xu, *Chem. Soc. Rev.*, 2006, **35**, 593–604.
42 D. Maspoch, D. Ruiz-Molina and J. Veciana, *Chem. Soc. Rev.*, 2007, **36**, 770–818.
43 G. Férey, *Chem. Soc. Rev.*, 2008, **37**, 191–214.
44 S. Lim, H. Kim, N. Selvapalam, K.-J. Kim, S. J. Cho, G. Seo and K. Kim, *Angew. Chem., Int. Ed.*, 2008, **47**, 3352–3355.
45 M. Eddaoudi, D. B. Moler, H. Li, B. Chen, T. M. Reineke, M. O'Keeffe and O. M. Yaghi, *Acc. Chem. Res.*, 2001, **34**, 319–330.
46 J. L. C. Rowsell and O. M. Yaghi, *Microporous Mesoporous Mater.*, 2004, **73**, 3–14.
47 G. Férey, *Stud. Surf. Sci. Catal.*, 2007, **170**, 66–86.
48 S. Kitagawa, R. Kitaura and S. Noro, *Angew. Chem., Int. Ed.*, 2004, **43**, 2334–2375.
49 S. Ma and H.-C. Zhou, *J. Am. Chem. Soc.*, 2006, **128**, 11734–11735.
50 D. F. Sava, V. C. Kravtsov, F. Nouar, L. Wojtas, J. F. Eubank and M. Eddaoudi, *J. Am. Chem. Soc.*, 2008, **130**, 3768–3770.
51 H. Li, M. Eddaoudi, M. O'Keeffe and O. M. Yaghi, *Nature*, 1999, **402**, 276–279.
52 R. Kitaura, S. Kitagawa, Y. Kubota, T. C. Kobayashi, K. Kindo, Y. Mita, A. Matsuo, M. Kobayashi, H.-C. Chang, T. C. Ozawa, M. Suzuki, M. Sakata and M. Takata, *Science*, 2002, **298**, 2358–2361.
53 G. Ferey, C. Mellot-Draznieks, C. Serre, F. Millange, J. Dutour, S. Surble and I. Margiolaki, *Science*, 2005, **309**, 2040–2042.
54 O. M. Yaghi, M. O'Keeffe, N. W. Ockwig, H. K. Chae, M. Eddaoudi and J. Kim, *Nature*, 2003, **423**, 705–714.
55 B. Moulton and M. J. Zaworotko, *Chem. Rev.*, 2001, **101**, 1629–1658.
56 M. J. Zaworotko, *Chem. Commun.*, 2001, 1–9.
57 O. R. Evans and W. Lin, *Acc. Chem. Res.*, 2002, **35**, 511–522.
58 M. J. Rosseinsky, *Microporous Mesoporous Mater.*, 2004, **73**, 15–30.
59 G. S. Papaefstathiou and L. R. MacGillivray, *Coord. Chem. Rev.*, 2003, **246**, 169–184.
60 L. Brammer, *Chem. Soc. Rev.*, 2004, **33**, 476–489.
61 R. J. Hill, D.-L. Long, N. R. Champness, P. Hubberstey and M. Schröeder, *Acc. Chem. Res.*, 2005, **38**, 335–348.
62 S. Kitagawa, S. Noro and T. Nakamura, *Chem. Commun.*, 2006, 701–707.
63 M. Hong, *Cryst. Growth Des.*, 2007, **7**, 10–14.
64 Y.-F. Song and L. Cronin, *Angew. Chem., Int. Ed.*, 2008, **47**, 4635–4637.
65 M. J. Zaworotko, *Nature*, 2008, **451**, 410–411.
66 M. P. Suh, Y. E. Cheon and E. Y. Lee, *Coord. Chem. Rev.*, 2008, **252**, 1007–1026.
67 U. Mueller, M. Schubert, F. Teich, H. Puetter, K. Schierle-Arndt and J. Pastré, *J. Mater. Chem.*, 2006, **16**, 626–636.
68 D. Britt, D. Tranchemontagne and O. M. Yaghi, *Proc. Natl. Acad. Sci. U. S. A.*, 2008, **105**, 11623–11627.
69 O. M. Yaghi, H. Li, C. Davis, D. Richardson and T. L. Groy, *Acc. Chem. Res.*, 1998, **31**, 474–484.
70 S. Kitagawa and M. Kondo, *Bull. Chem. Soc. Jpn.*, 1998, **71**, 1739–1753.
71 S. Kitagawa and K. Uemura, *Chem. Soc. Rev.*, 2005, **34**, 109–119.
72 A. J. Fletcher, K. M. Thomas and M. J. Rosseinsky, *J. Solid State Chem.*, 2005, **178**, 2491–2510.
73 E. Y. Lee, S. Y. Jang and M. P. Suh, *J. Am. Chem. Soc.*, 2005, **127**, 6374–6381.
74 B. D. Chandler, D. T. Cramb and G. K. H. Shimizu, *J. Am. Chem. Soc.*, 2006, **128**, 10403–10412.
75 W. J. Rieter, K. M. L. Taylor, H. An, W. Lin and W. Lin, *J. Am. Chem. Soc.*, 2006, **128**, 9024–9025.
76 J.-R. Li, Y. Tao, Q. Yu and X.-H. Bu, *Chem. Commun.*, 2007, 1527–1529.
77 Y. Liu, G. Li, X. Li and Y. Cui, *Angew. Chem., Int. Ed.*, 2007, **46**, 6301–6304.
78 G. J. Halder, C. J. Kepert, B. Moubaraki, K. S. Murray and J. D. Cashion, *Science*, 2002, **298**, 1762–1765.
79 D. Maspoch, D. Ruiz-Molina and J. Veciana, *J. Mater. Chem.*, 2004, **14**, 2713–2723.
80 P. D. C. Dietzel, Y. Morita, R. Blom and H. Fjellvaag, *Angew. Chem., Int. Ed.*, 2005, **44**, 6354–6358.
81 W. Ouellette, M. H. Yu, C. J. O'Connor, D. Hagrman and J. Zubieta, *Angew. Chem., Int. Ed.*, 2006, **45**, 3497–3500.
82 C. Yu, S. Ma, M. J. Pechan and H.-C. Zhou, *J. Appl. Phys.*, 2007, **101**, 09E108/101–09E108/103.
83 X.-M. Zhang, Z.-M. Hao, W.-X. Zhang and X.-M. Chen, *Angew. Chem., Int. Ed.*, 2007, **46**, 3456–3459.
84 Z. Wang, Y. Zhang, T. Liu, M. Kurmoo and S. Gao, *Adv. Funct. Mater.*, 2007, **17**, 1523–1536.
85 T. Okubo, R. Kawajiri, T. Mitani and T. Shimoda, *J. Am. Chem. Soc.*, 2005, **127**, 17598–17599.
86 Q. Ye, Y.-M. Song, G.-X. Wang, K. Chen, D.-W. Fu, P. W. H. Chan, J.-S. Zhu, S. D. Huang and R.-G. Xiong, *J. Am. Chem. Soc.*, 2006, **128**, 6554–6555.
87 Z. Xu, *Coord. Chem. Rev.*, 2006, **250**, 2745–2757.
88 M. Alvaro, E. Carbonell, B. Ferrer, F. X. Llabres i Xamena and H. Garcia, *Chem.–Eur. J.*, 2007, **13**, 5106–5112.
89 A. Kuc, A. Enyashin and G. Seifert, *J. Phys. Chem. B*, 2007, **111**, 8179–8186.
90 W. Lin, *J. Solid State Chem.*, 2005, **178**, 2486–2490.
91 R.-Q. Zou, H. Sakurai, S. Han, R.-Q. Zhong and Q. Xu, *J. Am. Chem. Soc.*, 2007, **129**, 8402–8403.
92 S. Horike, M. Dincă, K. Tamaki and J. R. Long, *J. Am. Chem. Soc.*, 2008, **130**, 5854–5855.
93 F. X. Llabrés i Xamena, O. Casanova, R. Galiasso Tailleur, H. Garcia and A. Corma, *J. Catal.*, 2008, **255**, 220–227.
94 U. Mueller, M. M. Schubert and O. M. Yaghi, *Handbook of Heterogeneous Catalysis*, Wiley-VCH, Weinheim, 2nd edn, 2008, **1**, pp. 247–262.
95 B. F. Hoskins and R. Robson, *J. Am. Chem. Soc.*, 1990, **112**, 1546–1554.
96 G. B. Gardner, D. Venkataraman, J. S. Moore and S. Lee, *Nature*, 1995, **374**, 792–795.
97 E. Lee, J. Kim, J. Heo, D. Whang and K. Kim, *Angew. Chem., Int. Ed.*, 2001, **40**, 399–402.
98 M. D. Ward, *Science*, 2003, **300**, 1104–1105.
99 J. L. C. Rowsell and O. M. Yaghi, *Angew. Chem., Int. Ed.*, 2005, **44**, 4670–4679.
100 X. Lin, J. Jia, P. Hubberstey, M. Schröder and N. R. Champness, *CrystEngComm*, 2007, **9**, 438–448.
101 D. J. Collins and H.-C. Zhou, *J. Mater. Chem.*, 2007, **17**, 3154–3160.
102 R. E. Morris and P. S. Wheatley, *Angew. Chem., Int. Ed.*, 2008, **47**, 4966–4981.

103 S. Q. Ma, D. Sun, J. M. Simmons, C. D. Collier, D. Yuan and H.-C. Zhou, *J. Am. Chem. Soc.*, 2008, **130**, 1012–1016.
104 M. Dincă and J. R. Long, *Angew. Chem., Int. Ed.*, 2008, **47**, 6766–6779.
105 O. M. Yaghi, G. Li and H. Li, *Nature*, 1995, **378**, 703–706.
106 Q. M. Wang, D. Shen, M. Bulow, M. L. Lau, S. Deng, F. R. Fitch, N. O. Lemcoff and J. Semanscin, *Microporous Mesoporous Mater.*, 2002, **55**, 217–230.
107 R. Custelcean and B. A. Moyer, *Eur. J. Inorg. Chem.*, 2007, 1321–1340.
108 The related literatures of selective gas adsorption and separation in this review.
109 B. Zhao, X.-Y. Chen, P. Cheng, D.-Z. Liao, S.-P. Yan and Z.-H. Jiang, *J. Am. Chem. Soc.*, 2004, **126**, 15394–15395.
110 B. Chen, Y. Yang, F. Zapata, G. Lin, G. Qian and E. B. Lobkovsky, *Adv. Mater.*, 2007, **19**, 1693–1696.
111 B. Chen, L. Wang, F. Zapata, G. Qian and E. B. Lobkovsky, *J. Am. Chem. Soc.*, 2008, **130**, 6718–6719.
112 B. V. Harbuzaru, A. Corma, F. Rey, P. Atienzar, J. L. Jorda, H. Garcia, D. Ananias, L. D. Carlos and J. Rocha, *Angew. Chem., Int. Ed.*, 2008, **47**, 1080–1083.
113 T. Uemura, R. Kitaura, Y. Ohta, M. Nagaoka and S. Kitagawa, *Angew. Chem., Int. Ed.*, 2006, **45**, 4112–4116.
114 C. J. Chuck, M. G. Davidson, M. D. Jones, G. Kociok-Köehn, M. D. Lunn and S. Wu, *Inorg. Chem.*, 2006, **45**, 6595–6597.
115 T. Uemura, D. Hiramatsu, Y. Kubota, M. Takata and S. Kitagawa, *Angew. Chem., Int. Ed.*, 2007, **46**, 4987–4990.
116 P. Horcajada, C. Serre, M. Vallet-Regí, M. Sebban, F. Taulelle and G. Férey, *Angew. Chem., Int. Ed.*, 2006, **45**, 5974–5978.
117 M. Vallet-Regí, F. Balas and D. Arcos, *Angew. Chem., Int. Ed.*, 2007, **46**, 7548–7558.
118 P. Horcajada, C. Serre, G. Maurin, N. A. Ramsahye, F. Balas, M. Vallet-Regí, M. Sebban, F. Taulelle and G. Férey, *J. Am. Chem. Soc.*, 2008, **130**, 6774–6780.
119 R. Q. Snurr, J. T. Hupp and S. T. Nguyen, *AIChE J.*, 2004, **50**, 1090–1095.
120 L. Pan, K. M. Adams, H. E. Hernandez, X. Wang, C. Zheng, Y. Hattori and K. Kaneko, *J. Am. Chem. Soc.*, 2003, **125**, 3062–3067.
121 D. N. Dybtsev, H. Chun, S. H. Yoon, D. Kim and K. Kim, *J. Am. Chem. Soc.*, 2004, **126**, 32–33.
122 D. G. Samsonenko, H. Kim, Y. Sun, G.-H. Kim, H.-S. Lee and K. Kim, *Chem.–Asian J.*, 2007, **2**, 484–488.
123 M. Dincă and J. R. Long, *J. Am. Chem. Soc.*, 2005, **127**, 9376–9377.
124 R. Matsuda, R. Kitaura, S. Kitagawa, Y. Kubota, R. V. Belosludov, T. C. Kobayashi, H. Sakamoto, T. Chiba, M. Takata, Y. Kawazoe and Y. Mita, *Nature*, 2005, **436**, 238–241.
125 L. Pan, D. H. Olson, L. R. Ciemnolonski, R. Heddy and J. Li, *Angew. Chem., Int. Ed.*, 2006, **45**, 616–619.
126 S. Surblé, F. Millange, C. Serre, T. Düren, M. Latroche, S. Bourrelly, P. L. Llewellyn and G. Férey, *J. Am. Chem. Soc.*, 2006, **128**, 14889–14896.
127 T. Loiseau, L. Lecroq, C. Volkringer, J. Marrot, G. Férey, M. Haouas, F. Taulelle, S. Bourrelly, P. L. Llewellyn and M. Latroche, *J. Am. Chem. Soc.*, 2006, **128**, 10223–10230.
128 L. Pan, B. Parker, X. Y. Huang, D. H. Olson, J. Lee and J. Li, *J. Am. Chem. Soc.*, 2006, **128**, 4180–4181.
129 M. Dincă, A. F. Yu and J. R. Long, *J. Am. Chem. Soc.*, 2006, **128**, 8904–8913.
130 X. Lin, A. J. Blake, C. Wilson, X. Z. Sun, N. R. Champness, M. W. George, P. Hubberstey, R. Mokaya and M. Schröder, *J. Am. Chem. Soc.*, 2006, **128**, 10745–10753.
131 S. Q. Ma, X. S. Wang, C. D. Collier, E. S. Manis and H.-C. Zhou, *Inorg. Chem.*, 2007, **46**, 8499–8501.
132 Y. Zou, S. Hong, M. Park, H. Chun and M. S. Lah, *Chem. Commun.*, 2007, 5182–5184.
133 C.-J. Li, Z.-J. Lin, M.-X. Peng, J.-D. Leng, M.-M. Yang and M.-L. Tong, *Chem. Commun.*, 2008, 6348–6350.
134 J. Y. Lee, D. H. Olson, L. Pan, T. J. Emge and J. Li, *Adv. Funct. Mater.*, 2007, **17**, 1255–1262.
135 Y. Li and R. T. Yang, *Langmuir*, 2007, **23**, 12937–12944.
136 S. M. Humphrey, J.-S. Chang, S. H. Jhung, J. W. Yoon and P. T. Wood, *Angew. Chem., Int. Ed.*, 2007, **46**, 272–275.
137 J. W. Yoon, S. H. Jhung, Y. K. Hwang, S. M. Humphrey, P. T. Wood and J.-S. Chang, *Adv. Mater.*, 2007, **19**, 1830–1834.
138 J.-R. Li, Y. Tao, Q. Yu, X.-H. Bu, H. Sakamoto and S. Kitagawa, *Chem.–Eur. J.*, 2008, **14**, 2771–2776.
139 J. A. R. Navarro, E. Barea, A. Rodríguez-Diéguez, J. M. Salas, C. O. Ania, J. B. Parra, N. Masciocchi, S. Galli and A. Sironi, *J. Am. Chem. Soc.*, 2008, **130**, 3978–3984.
140 R. Banerjee, A. Phan, B. Wang, C. Knobler, H. Furukawa, M. O'Keeffe and O. M. Yaghi, *Science*, 2008, **319**, 939–943.
141 B. Wang, A. P. Côté, H. Furukawa, M. O'Keeffe and O. M. Yaghi, *Nature*, 2008, **453**, 207–211.
142 B. L. Chen, Y. Y. Ji, M. Xue, F. R. Fronczek, E. J. Hurtado, J. U. Mondal, C. D. Liang and S. Dai, *Inorg. Chem.*, 2008, **47**, 5543–5545.
143 M. Xue, S. Q. Ma, Z. Jin, R. M. Schaffino, G. S. Zhu, E. B. Lobkovsky, S. L. Qiu and B. L. Chen, *Inorg. Chem.*, 2008, **47**, 6825–6828.
144 H. R. Moon, N. Kobayashi and M. P. Suh, *Inorg. Chem.*, 2006, **45**, 8672–8676.
145 S. Q. Ma, X. S. Wang, D. Q. Yuan and H.-C. Zhou, *Angew. Chem., Int. Ed.*, 2008, **47**, 4130–4133.
146 Y.-S. Bae, O. K. Farha, A. M. Spokoyny, C. A. Mirkin, J. T. Hupp and R. Q. Snurr, *Chem. Commun.*, 2008, 4135–4137.
147 K. Li, D. H. Olson, J. Y. Lee, W. Bi, K. Wu, T. Yuen, Q. Xu and J. Li, *Adv. Funct. Mater.*, 2008, **18**, 2205–2214.
148 Y.-S. Bae, K. L. Mulfort, H. Frost, P. Ryan, S. Punnathanam, L. J. Broadbelt, J. T. Hupp and R. Q. Snurr, *Langmuir*, 2008, **24**, 8592–8598.
149 H. Kim, D. G. Samsonenko, M. Yoon, J. W. Yoon, Y. K. Hwang, J.-S. Chang and K. Kim, *Chem. Commun.*, 2008, 4697–4699.
150 S. Cavenati, C. A. Grande, A. E. Rodrigues, C. Kiener and U. Müller, *Ind. Eng. Chem. Res.*, 2008, **47**, 6333–6335.
151 A. Sartbaeva, S. A. Wells, M. M. J. Treacy and M. F. Thorpe, *Nat. Mater.*, 2006, **5**, 962–965.
152 D. I. Kopelevich and H. C. Chang, *J. Chem. Phys.*, 2001, **115**, 9519–9527.
153 N. E. R. Zimmermann, S. Jakobtorweihen, E. Beerdsen, B. Smit and F. J. Keil, *J. Phys. Chem. C*, 2007, **111**, 17370–17381.
154 Y. Lee, J. A. Hriljac, T. Vogt, J. B. Parise, M. J. Edmondson, P. A. Anderson, D. R. Corbin and T. Nagai, *J. Am. Chem. Soc.*, 2001, **123**, 8418–8419.
155 S. M. Kuznicki, V. A. Bell, S. Nair, H. W. Hillhouse, R. M. Jacubinas, C. M. Braunbarth, B. H. Toby and M. Tsapatsis, *Nature*, 2001, **412**, 720–724.
156 J. Plévert, T. M. Gentz, A. Laine, H. L. Li, V. G. Young, O. M. Yaghi and M. O'Keeffe, *J. Am. Chem. Soc.*, 2001, **123**, 12706–12707.
157 Y. Lee, T. Vogt, J. A. Hriljac, J. B. Parise, J. C. Hanson and S. J. Kim, *Nature*, 2002, **420**, 485–489.
158 R. Kitaura, K. Seki, G. Akiyama and S. Kitagawa, *Angew. Chem., Int. Ed.*, 2003, **42**, 428–431.
159 K. Seki, *Phys. Chem. Chem. Phys.*, 2002, **4**, 1968–1971.
160 R. Kitaura, K. Fujimoto, S. Noro, M. Kondo and S. Kitagawa, *Angew. Chem., Int. Ed.*, 2002, **41**, 133–135.
161 T. K. Maji, K. Uemura, H. C. Chang, R. Matsuda and S. Kitagawa, *Angew. Chem., Int. Ed.*, 2004, **43**, 3269–3272.
162 S. Bourrelly, P. L. Llewellyn, C. Serre, F. Millange, T. Loiseau and G. Férey, *J. Am. Chem. Soc.*, 2005, **127**, 13519–13521.
163 T. K. Maji, G. Mostafa, R. Matsuda and S. Kitagawa, *J. Am. Chem. Soc.*, 2005, **127**, 17152–17153.
164 P. L. Llewellyn, S. Bourrelly, C. Serre, Y. Filinchuk and G. Férey, *Angew. Chem., Int. Ed.*, 2006, **45**, 7751–7754.
165 B. L. Chen, S. Q. Ma, E. J. Hurtado, E. B. Lobkovsky and H.-C. Zhou, *Inorg. Chem.*, 2007, **46**, 8490–8492.
166 S. Q. Ma, X. S. Wang, E. S. Manis, C. D. Collier and H.-C. Zhou, *Inorg. Chem.*, 2007, **46**, 3432–3434.
167 H. Hayashi, A. P. Côté, H. Furukawa, M. O'Keeffe and O. M. Yaghi, *Nat. Mater.*, 2007, **6**, 501–506.
168 S. Hasegawa, S. Horike, R. Matsuda, S. Furukawa, K. Mochizuki, Y. Kinoshita and S. Kitagawa, *J. Am. Chem. Soc.*, 2007, **129**, 2607–2614.
169 T. K. Maji, R. Matsuda and S. Kitagawa, *Nat. Mater.*, 2007, **6**, 142–148.

170 S. K. Ghosh, J. P. Zhang and S. Kitagawa, *Angew. Chem., Int. Ed.*, 2007, **46**, 7965–7968.
171 B. L. Chen, S. Q. Ma, E. J. Hurtado, E. B. Lobkovsky, C. D. Liang, H. G. Zhu and S. Dai, *Inorg. Chem.*, 2007, **46**, 8705–8709.
172 B. L. Chen, S. Q. Ma, F. Zapata, F. R. Fronczek, E. B. Lobkovsky and H.-C. Zhou, *Inorg. Chem.*, 2007, **46**, 1233–1236.
173 D. Tanaka, K. Nakagawa, M. Higuchi, S. Horike, Y. Kubota, L. C. Kobayashi, M. Takata and S. Kitagawa, *Angew. Chem., Int. Ed.*, 2008, **47**, 3914–3918.
174 Y. E. Cheon and M. P. Suh, *Chem.–Eur. J.*, 2008, **14**, 3961–3967.
175 J. P. Zhang and X. M. Chen, *J. Am. Chem. Soc.*, 2008, **130**, 6010–6017.
176 S. K. Ghosh, S. Bureekaew and S. Kitagawa, *Angew. Chem., Int. Ed.*, 2008, **47**, 3403–3406.
177 P. K. Thallapally, J. Tian, M. R. Kishan, C. A. Fernandez, S. J. Dalgarno, P. B. McGrail, J. E. Warren and J. L. Atwood, *J. Am. Chem. Soc.*, 2008, **130**, 16842–16843.
178 S. Uchida, R. Kawamoto, H. Tagami, Y. Nakagawa and N. Mizuno, *J. Am. Chem. Soc.*, 2008, **130**, 12370–12376.
179 D. W. Breck, *J. Chem. Educ.*, 1964, **41**, 678–689.
180 M. M. Dubinin, K. M. Nikolaev, N. S. Polyakov and N. I. Seregina, *Izv. Akad. Nauk SSSR, Ser. Khim.*, 1971, 1871–1876.
181 S. Q. Ma, D. Sun, X. S. Wang and H. C. Zhou, *Angew. Chem., Int. Ed.*, 2007, **46**, 2458–2462.
182 S. Ma, J.-R. Li, R. Kuppler and H.-C. Zhou, unpublished work.
183 A. R. Leach, *Molecular Modelling Principles and Applications*, Prentice Hall, London, 2nd edn., 2001.
184 J. Jiang and S. I. Sandler, *Langmuir*, 2006, **22**, 5702–5707.
185 L. Zhang, Q. Wang, T. Wu and Y.-C. Liu, *Chem.–Eur. J.*, 2007, **13**, 6387–6396.
186 T. Düren and R. Q. Snurr, *J. Phys. Chem. B*, 2004, **108**, 15703–15708.
187 B. Liu, Q. Yang, C. Xue, C. Zhong, B. Chen and B. Smit, *J. Phys. Chem. C*, 2008, **112**, 9854–9860.
188 T. M. Nicholson and S. K. Bhatia, *J. Phys. Chem. B*, 2006, **110**, 24834–24836.
189 S. Wang, Q. Yang and C. Zhong, *Sep. Purif. Technol.*, 2008, **60**, 30–35.
190 Q. Yang, C. Xue, C. Zhong and J.-F. Chen, *AIChE J.*, 2007, **53**, 2832–2840.
191 J. R. Karra and K. S. Walton, *Langmuir*, 2008, **24**, 8620–8626.
192 Q. Yang and C. Zhong, *J. Phys. Chem. B*, 2006, **110**, 17776–17783.
193 Q. Yang and C. Zhong, *ChemPhysChem*, 2006, **7**, 1417–1421.
194 D. Dubbeldam, C. J. Galvin, K. S. Walton, D. E. Ellis and R. Q. Snurr, *J. Am. Chem. Soc.*, 2008, **130**, 10884–10885.
195 F. Stallmach, S. Gröeger, V. Kuenzel, J. Käerger, O. M. Yaghi, M. Hesse and U. Müller, *Angew. Chem., Int. Ed.*, 2006, **45**, 2123–2126.
196 N. Rosenbach, Jr, H. Jobic, A. Ghoufi, F. Salles, G. Maurin, S. Bourrelly, L. Llewellyn Philip, T. Devic, C. Serre and G. Férey, *Angew. Chem., Int. Ed.*, 2008, **47**, 6611–6615.
197 A. I. Skoulidas, *J. Am. Chem. Soc.*, 2004, **126**, 1356–1357.
198 A. I. Skoulidas and D. S. Sholl, *J. Phys. Chem. B*, 2005, **109**, 15760–15768.
199 L. Sarkisov, T. Dueren and R. Q. Snurr, *Mol. Phys.*, 2004, **102**, 211–221.
200 R. Babarao and J. Jiang, *Langmuir*, 2008, **24**, 5474–5484.
201 V. Krungleviciute, K. Lask, A. D. Migone, J. Y. Lee and J. Li, *AIChE J.*, 2008, **54**, 918–923.
202 M. Hartmann, S. Kunz, D. Himsl and O. Tangermann, *Langmuir*, 2008, **24**, 8634–8642.
203 A. Méthivier, in *Zeolites for Cleaner Technologies*, ed. M. Guisnet and J.-P. Gilson, Imperial College Press, London, 2002.
204 L. Alaerts, C. E. A. Kirshhock, M. Maes, M. A. van der Veen, V. Finsy, A. Depla, J. A. Martens, G. V. Baron, P. A. Jacobs, J. F. M. Denayer and D. E. De Vos, *Angew. Chem., Int. Ed.*, 2007, **46**, 4293–4297.
205 V. Finsy, H. Verelst, L. Alaerts, D. De Vos, P. A. Jacobs, G. V. Baron and J. F. M. Denayer, *J. Am. Chem. Soc.*, 2008, **130**, 7110–7118.
206 L. Alaerts, M. Maes, L. Giebeler, P. A. Jacobs, J. A. Martens, J. F. M. Denayer, C. E. A. Kirschhock and D. E. De Vos, *J. Am. Chem. Soc.*, 2008, **130**, 14170–14178.
207 S. W. Sohn, *Kerosene ISOSIV Process for Production of Normal Paraffins, in Handbook of Petroleum Refining Processes*, ed. R. A. Meyers, McGraw-Hill, New York, 3rd edn., 2004.
208 P. S. Bárcia, F. Zapata, J. A. C. Silva, A. E. Rodrigues and B. Chen, *J. Phys. Chem. B*, 2007, **111**, 6101–6103.
209 S. Kulprathipanja and R. W. Neuzil, US Patent 4 445 444, 1984, UOP, [*Chem. Abs.* 101, 75824].
210 B. Chen, C. Liang, J. Yang, D. S. Contreras, Y. L. Clancy, E. B. Lobkovsky, O. M. Yaghi and S. Dai, *Angew. Chem., Int. Ed.*, 2006, **45**, 1390–1393.
211 N. Y. Chen, W. E. Garwood and F. G. Dwyer, *Shape-Selective Catalysis in Industrial Applications*, Marcel Dekker, New York, 1989.
212 C. M. White, D. H. Smith, K. L. Jones, A. L. Goodman, S. A. Jikich, R. B. LaCount, S. B. DuBose, E. Ozdemir, B. I. Morsi and K. T. Schroeder, *Energy Fuels*, 2005, **19**, 659–724.
213 *IPCC Special Report on: Carbon Dioxide Capture and Storage*, 2005. Available *via* the Internet at http://www.ipcc.ch/.
214 L. Bastin, P. S. Barcia, E. J. Hurtado, J. A. C. Silva, A. E. Rodrigues and B. Chen, *J. Phys. Chem. C*, 2008, **112**, 1575–1581.
215 H. Tanaka, H. Kanoh, M. Yudasaka, S. Iijima and K. Kaneko, *J. Am. Chem. Soc.*, 2005, **127**, 7511–7516.
216 X. Zhao, S. Villar-Rodil, A. J. Fletcher and K. M. Thomas, *J. Phys. Chem. B*, 2006, **110**, 9947–9955.
217 A. V. A. Kumar and S. K. Bhatia, *Phys. Rev. Lett.*, 2005, **95**, 245901–245904.
218 Y. Hattori, H. Tanaka, F. Okino, H. Touhara, Y. Nakahigashi, S. Utsumi, H. Kanoh and K. Kaneko, *J. Phys. Chem. B*, 2006, **110**, 9764–9767.
219 B. Chen, X. Zhao, A. Putkham, K. Hong, E. B. Lobkovsky, E. J. Hurtado, A. J. Fletcher and K. M. Thomas, *J. Am. Chem. Soc.*, 2008, **130**, 6411–6423.
220 D. Noguchi, H. Tanaka, A. Kondo, H. Kajiro, H. Noguchi, T. Ohba, H. Kanoh and K. Kaneko, *J. Am. Chem. Soc.*, 2008, **130**, 6367–6372.
221 Y. Yampolskii, I. Pinnau and B. D. Freeman, *Materials Science of Membranes for Gas and Vapor Separation*, John Wiley & Sons Ltd., West Sussex, 2006.
222 E. E. McLeary, J. C. Jansen and F. Kapteijn, *Microporous Mesoporous Mater.*, 2006, **90**, 198–220.
223 H. Guo, G. Zhu, I. J. Hewitt and S. Qiu, *J. Am. Chem. Soc.*, 2009, **131**, 1646–1647.
224 S. Keskin and D. S. Sholl, *J. Phys. Chem. C*, 2007, **111**, 14055–14059.
225 J. Won, J. S. Seo, J. H. Kim, H. S. Kim, Y. S. Kang, S.-J. Kim, Y. Kim and J. Jegal, *Adv. Mater.*, 2005, **17**, 80–84.
226 A. Car, C. Stropnik and K.-V. Peinemann, *Desalination*, 2006, **200**, 424–426.
227 E. V. Perez, K. J. Balkus, Jr, J. P. Ferraris and I. H. Musselman, *J. Membr. Sci.*, 2009, **328**, 165–173.